

Waste Sector: Estimating CH₄ Emissions from Solid Waste Disposal Sites



Hugh Runyan^{1,3}, Yuchen Wu^{1,3}, Andre Scheinwald^{1,3},
Yuan (Rose) Wang^{1,3*}, Tom Frankiewicz^{1,3},
John McGrath^{1,3}, and Krsna Raniga^{2,3}

1) RMI, 2) WattTime, 3) Climate TRACE

* Email address: rwang@rmi.org

1. Introduction

Methane (CH₄) is a potent greenhouse gas responsible for 30% of global warming since the industrial revolution and is 28 times more potent than carbon dioxide over a 100-year timespan (Ayandele et al., 2022). Solid waste disposal sites (SWDS) are the third largest human-generated source responsible for increasing atmospheric methane worldwide, after fossil fuels and enteric fermentation. SWDS accounted for 12% of total global anthropogenic methane emissions in 2024 (IEA, 2024; UNEP/CCAC, 2022). In the United States, SWDS contribute 14.5% of greenhouse gas generation (EPA, 2022). Emissions from SWDS are generated by anaerobic decomposition of organic waste.

Globally, 37% of waste is landfilled, while 33% is openly dumped, 19% is diverted before reaching SWDS, and 11% is incinerated for energy recovery (Kaza et al., 2018). Definitions and management standards of SWDS vary widely by income level. Sanitary landfills are engineered facilities designed with liners, leachate control, and often methane capture, whereas open dumpsites are uncontrolled waste disposal areas lacking environmental safeguards. In low-income countries, roughly 93% of waste is openly dumped, with limited collection coverage, access to controlled landfilling, or centralized waste treatment (Kaza et al., 2018).

Data on SWDS, which is crucial for understanding and mitigating methane emissions, are frequently fragmented, inconsistent, or incomplete. While a few countries provide site-level methane emissions data—such as the U.S. Environmental Protection Agency's (EPA) Greenhouse Gas Reporting Program (GHGRP), the European Pollutant Release and Transfer Register (E-PRTR), and Canada's Greenhouse Gas Reporting Program (Canada GHGRP)—these remain the exception rather than the rule. Most countries do not report at this level of granularity, leaving significant gaps in global coverage. Moreover, the U.S. EPA issued a proposed rule in September 2025 to reconsider the GHGRP. The proposal would remove reporting requirements for multiple source categories, including municipal solid waste landfills (Subpart HH), as part of a broader effort to streamline or suspend reporting obligations until 2034 (U.S. EPA, 2025b), which would further limit the availability of facility-level reported data. However, this rule has

not yet been finalized, and landfill facilities remain obligated to report under the current GHGRP framework, as of October 2025, until a final decision is published. Similarly, the EPA’s Landfill Methane Outreach Program (LMOP), Mexico’s National Institute of Statistics and Geography (INEGI), and Brazil’s National Solid Waste Management Information System (SINIR) offer insights into waste quantities and management practices, but the absence of direct emissions data limits their utility in creating a comprehensive emissions profile.

Global-scale data collection efforts like OpenStreetMap (OSM), though broad in scope, suffer from issues of verification. A small sample of cataloged OSM SWDS we examined contained incorrectly labeled sites. Global Plastic Watch introduced a novel approach employing satellite remote sensing to identify plastic-rich waste sites all over the globe, but its focus on plastic might overlook SWDS with low plastic content. Waste Atlas (another global catalog) is outdated, having last been updated in 2013.

Considering the complexity of the waste data landscape, the 2025 Climate TRACE methodology for national and asset-level emissions estimation uses a three-step approach: 1) Aggregate and deduplicate waste disposal sites data from various sources; 2) Fill gaps in input sources with modeled values or IPCC defaults; 3) Emissions estimation, which comprises multiple pathways depending on site-specific data availability. The methodology is outlined below.

Based on the asset-level emissions estimates, the authors also recommend emissions reduction solutions (ERSs) for each SWDS based on site type, economic conditions of the country where each SWDS is located, and other available site-specific information to demonstrate the methane mitigation potential of implementing increased waste diversion from disposal sites as well as improved site management practices.

2. Materials and Methods

Waste datasets were selected based on comprehensive data availability for three key parameters: surface area, annual incoming waste, and methane emissions data from self-reported programs and remote sensing measurements. Where none of these were available, the SWDS was omitted from the final composite dataset. The composite dataset was contingent on a combination of data richness, source reliability, and recency, where a hierarchy of preference in data source was implemented if multiple datasets overlapped on certain SWDS (see Section 2.1.4).

A major change in this year’s Climate TRACE methodology is the adoption of a mechanistic first-order decay (FOD) model for estimating methane emissions. The advantage of this approach lies in its improved interpretability – making it easier to understand the driving forces behind emissions. In addition, it enables the design of more targeted emissions reduction strategies, as the model can leverage site-specific data to inform actionable mitigation pathways.

A Python version of EPA's Solid Waste Emissions Estimation Tool (SWEET) created by RMI (RMI, 2025) is used as the backbone of modeling. Where satellite or reported emissions data were available, parameter calibration or data fusion was used to account for those. A high-level overview of Climate TRACE's 2025 approach is shown in Figure 3.

2.1 Constructing the Facility Waste Dataset

Constructing the facility dataset required pre-processing and integrating a variety of solid waste data sources, which varied in their completeness and geographical coverage. The primary goal was to construct a unified dataset composed of unique waste sites, while incorporating the most comprehensive information available per location. The datasets were constructed in the following stages:

1. Pre-modeling inventory: This stage involved creating a deduplicated, filtered concatenation of all individual contributing datasets, deploying a hierarchy of source preference when multiple sources reported on the same site. A unique asset identifier was assigned to each site.
2. Plume matching: In this stage, satellite plume data were spatially matched with waste sites.
3. Final dataset: This stage involved filling data gaps with modeled or default values. Incoming waste amount data were filled where needed by the area-to-incoming-waste model (section 2.2.2), and parameters such as methane correction factors, unavailable in any dataset, were filled with IPCC country-level or regional defaults.

2.1.1 Core datasets employed

U.S. EPA GHGRP: The U.S. EPA's Greenhouse Gas Reporting Program (GHGRP) requires over 8,000 large-emitter facilities (>25,000 megatons CO₂ equivalent annually) to report their greenhouse gas emissions each year (US EPA, 2025a). This is the broadest and most comprehensive dataset publicly available on U.S. waste disposal sites. The reported data was acquired through the EPA's GraphQL API (<https://enviro.epa.gov/query-builder/ghg>), which includes data such as annual accepted waste, emissions, and cover types from 2010-2023).

U.S. EPA LMOP: SWDS data were collected from the Landfill Methane Outreach Program (LMOP; <https://www.epa.gov/lmop>), whose sources include facility self-reports and partner reports, and data are publicly available (US EPA, 2025b). Beyond surface area, waste-in-place, annual capacity, and operating years, many sites published landfill gas generation (LFG) and collection values. For US sites that did not meet the EPA's GHGRP criteria, the net published LFG values (LFG generated minus LFG collected) in LMOP data were utilized to estimate methane emissions.

Canada GHGRP: Similar to the U.S. EPA GHGRP, Canada requires annual reports from facilities that emit at least 10,000 tons of carbon dioxide equivalent per year (<https://www.canada.ca/en/environment-climate-change/services/climate-change/greenhouse-gas>

-emissions/facility-reporting/data.html). 133 unique locations reported emissions between 2004-2021. The program only publishes annual emissions quantities and ownership information (Government of Canada, 2025).

E-PRTR: The European Pollutant Release and Transfer Register reports pollutant releases, including greenhouse gas emissions, from industrial facilities in the European Union (EU, 2025; <https://industry.eea.europa.eu/>). Between 2007 and 2021, 1,426 landfills reported emissions. The E-PRTR only publishes landfill locations and annual emissions quantities.

INEGI: Mexico's National Institute of Statistics and Geography (INEGI) published landfill locations, waste quantities, and practices in 2017 under its “National Census of Municipal and Delegational Governments 2017” (Mexico National Institute of Statistics and Geography (INEGI), 2017; <https://en.www.inegi.org.mx/>). This dataset reports on 2,204 active landfills since 2016, and publishes information including their opening dates, annual incoming waste, existence of landfill cover, and existence of gas collection systems.

Waste Atlas: This dataset is presented as an interactive map with data compiled through crowdsourcing and scientific research for 2013 (Waste Atlas, 2013; <http://www.atlas.d-waste.com/>). The information available per location is a mix of waste-in-place, annual capacity, and operating status. Between sanitary landfills and dumpsites, there are 662 unique locations.

OpenStreetMap: The OpenStreetMap (OSM) dataset is composed of labels, locations, and areas (OpenStreetMap Foundation, 2025; <https://www.openstreetmap.org>). This dataset contained 12,272 locations tagged as “landuse = landfill” that were larger than 10 m². It is important to note that not every location in this dataset was confirmed as a SWDS. Due to the dataset's size and the visual similarities between SWDS and some other types of facilities, manual verification was impractical. The team is progressively removing sites that do not appear to be waste sites through high-res satellite imagery and greatly appreciates partners, such as researchers in UNEP's International Methane Emissions Observatory (IMEO) program, for their support on this process.

SINIR: The Sistema Nacional de Informações sobre a Gestão dos Resíduos Sólidos (SINIR) is publicly available data collected by the Federative Republic of Brazil (Federative Republic of Brazil, 2019; <https://relatorios.sinir.gov.br/relatorios/municipal/>). The data is a time series of 3,914 landfills from 2014-2019. It includes information such as landfill locations (generally just city center geocoordinates), annual incoming waste, landfill type, and open and close dates.

CATF: The Clean Air Task Force (Clean Air Task Force (CATF), 2025; <https://www.catf.us/>) data were provided by CATF through their country engagement work in Mexico and Ecuador. The dataset is a time series of 4 landfills from 2012-2023; it includes fields such as landfill

locations, annual incoming waste, waste in place, facility cover, percent coverage, and waste composition.

Global Plastic Watch (GPW): This database consists of plastic-containing waste sites identified by a system of neural networks created to analyze spectral, spatial, and temporal components of Sentinel-2 satellite data to find terrestrial waste aggregations (Global Plastic Watch, 2021). Following identification, the footprint of each site was calculated and monitored at monthly intervals. This approach has detected nearly 1,738 waste sites over 1,000 m² in 26 countries (Figure 1). The GPW method generated contours to estimate the areas of detected waste aggregations, updated at a monthly cadence from the Sentinel-2 observation period between 2017 and early-2021. As no specific timestamp was available for each site when the data was downloaded to use for this work, all areas were treated as 2021 data.



Figure 1. An example of a large waste site in Indonesia as shown on GPW, showing available site attributes when selected (top left corner of the image) and the countries with locations identified in yellow (inset right).

2.1.2 Supplemental datasets:

World Bank: The World Bank's "What a Waste 2.0: A Global Snapshot of Solid Waste Management to 2050" report highlights regional and global solid waste generation, management, and impact trends (Kaza et al., 2018; <https://datatopics.worldbank.org/what-a-waste/>). Regional annual waste generation growth rates were derived from the report and used to project capacities to 2024, forming the basis for constructing the pre-modeling and final inventories (see Section

2.1.4). For the capacity modeling stage, the following income groups were assigned to each site by country, per the report's categories: low-income, lower-middle income, upper-middle income, and high-income. For the emissions modeling stage, the following region groups were assigned to each site by country, per the report's categories: East Asia & Pacific, South Asia, Europe & Central Asia, Middle East & North Africa, Sub-Saharan Africa, North America, Latin America & the Caribbean.

WorldClim: The methane generation rate constant (k-value) was calculated using precipitation and temperature data based on the methodology published by Wang et al. (2024). Facility geocoordinates were used to find the nearest weather data. This data is sourced from WorldClim and covers 2000-2021 (WorldClim, 2025; <https://www.worldclim.org/>).

United Nations Population Data: Population growth rates are used to estimate changes in variables such as waste generation rates through time. The population data comes from the UN Population Division, Department of Economic and Social Affairs (United Nations, Department of Economic and Social Affairs, Population Division, 2025; <https://population.un.org/dataportal/>).

2.1.3 Remote Sensing Data

Carbon Mapper

The Carbon Mapper Open Data Portal provides plume detections from various sensors located on different platforms from air- and spaceborne. The following sensors, totals plumes, and date ranges were accessed:

Tanager - 3,574 plumes from 9/19/2024 - 5/7/2025.

ISS: EMIT – 4,649 plumes from 8/10/2022 - 4/21/2025

Global Airborne Observatory – 9,743 plumes from 10/10/2019 - 6/12/2024

AVIRIS (Airborne Visible InfraRed Imaging Spectrometer) campaigns – 5,613 plumes from 9/10/2016 - 3/19/2023

Only plumes spatially matched to a known SWDS were used. Plume uncertainties and wind data were also available for each observation (Carbon Mapper, Inc., 2025; <https://carbonmapper.org/>).

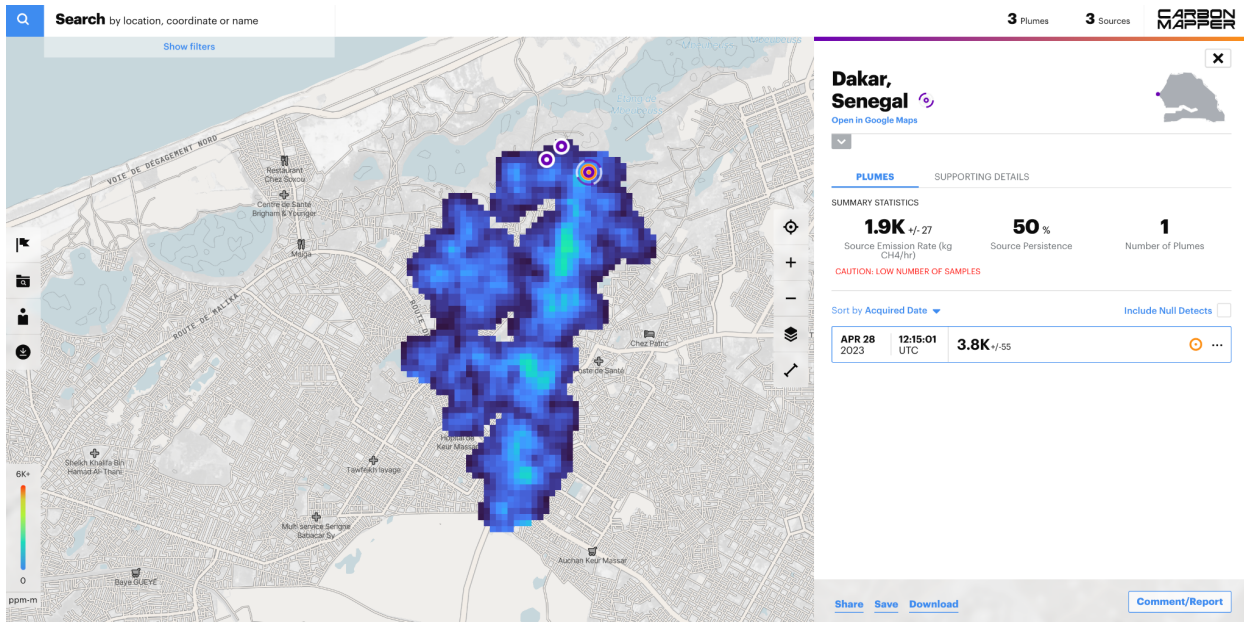


Figure 2. A methane plume example from a waste site (landfill) in Senegal from the Carbon Mapper website.

SRON/GHGSat: A total of 594 satellite plume detections were available from SRON's TWOS initiative (Space Research Organisation Netherlands Targeting Waste emissions Observed from Space) spanning from 9/22/2020-3/30/2025 (Maasakkers & Aben, 2025 <https://www.sron.nl/en/pillars/science/earth/targeting-waste-emissions-observed-from-space/>). Plumes were only used if spatially matched to known SWDS. Original plume imagery is from GHGSat satellites (GHGSat, 2025; <https://www.ghgsat.com/>).

IMEO: We ingested 195 additional EnMAP (Environmental Mapping and Analysis Program) plumes from the International Methane Emissions Observatory (IMEO) data portal, with 21 identified as coal mining, 171 oil & gas, and 3 from solid waste (UNEP, 2025; <https://www.unep.org/topics/energy/methane/international-methane-emissions-observatory>). The data spans from 3/19/2023-12/26/2024. Plumes were only used if spatially matched to a known waste site.

2.1.4 Filtering & deduplication for the pre-modeling inventory

In order to create a harmonized SWDS inventory, sources reporting direct emissions were prioritized, such as the EPA datasets, Canada GHGRP, and E-PRTR. When reconciling overlapping data from the LMOP and EPA GHGRP datasets, GHGRP data were preferred because they contain directly reported emissions estimates.

OSM sites smaller than 10,000 square meters were excluded to filter out potential false positives. The threshold for GPW sites was set lower—1,000 square meters—due to the greater reliability of GPW's remote-sensing techniques. Further refinement on OSM data required first decoding

Unicode contents in the JSON labels and translating non-English labels. Sites were removed based on a list of keywords for non-MSW identifiers, such as “construction” or “tailings”.

Spatial deduplication was necessary both within source datasets and between them. The initial composite dataset, concatenated from all the individual contributing datasets, was spatially matched to itself using a clustering recursion in Postgres using PostGIS. The largest overlapping site (based on a 1,500-meter radius) from the same source was retained. For datasets with no reported areas, OSM areas from matching locations were used.

Finally, OSM, GPW, and Waste Atlas sites overlapping with locations from more informative sources like EPA GHGRP, EPA LMOP, Canada GHGRP, E-PRTR, and INEGI were merged to fill in gaps. Consequently, a single waste site in the final training datasets could encompass multi-source data, including area, capacity, and emissions.



Figure 3. Waste emission modeling flowchart.

2.2 Model development

An overview of the Climate TRACE solid waste methane emissions estimation process is illustrated in Figure 3. Beginning at the top of the flow chart, if the source datasets for the site included reported emissions, those emission estimates were projected to a time series using average country-level historical and projected future population growth rates. This modeling pathway will be referred to as the no-FOD pathway (top-right of flowchart), with FOD standing for first-order decay. Details of the projection methodology are provided in Section 2.2.1.

Where emissions estimates were not reported, they were generated through a two-stage estimation process referred to as the FOD pathway (top-left of flowchart). First, when annual incoming waste values were unavailable, they were estimated using a modeled relationship

between landfill surface area and annual incoming waste. This model, referred to as the area-to-incoming-waste model, is described in section 2.2.2. Second, the Python implementation of the US EPA SWEET model was used to estimate methane emissions from incoming waste and other source dataset parameters (RMI, 2025; Solid Waste Emissions Estimation Tool (SWEET) | Global Methane Initiative, 2025). Where reported values were missing, IPCC country-level or regional default parameters were applied. Because SWEET is a first-order decay model, this modeling approach is referred to as the FOD pathway, and it is explained in more depth in section 2.2.3.

After the input data went through the above two pathways, all landfills with adequate source data had associated emissions estimates. If Carbon Mapper provided methane plume measurements at a site were available for at least 5 months, they were used to inform and update the emissions estimates in one of two ways:

- 1) Incoming waste calibration: For landfills that initially used the area-to-incoming-waste model, satellite measurements were used to re-estimate new annual incoming waste values due to the relatively large uncertainty in the area-to-incoming-waste model.
- 2) Scale factor fusion: For all other landfills, emissions estimates were combined with satellite measurements through an uncertainty-informed fusion process.

This satellite stage is described in detail in section 2.2.4.

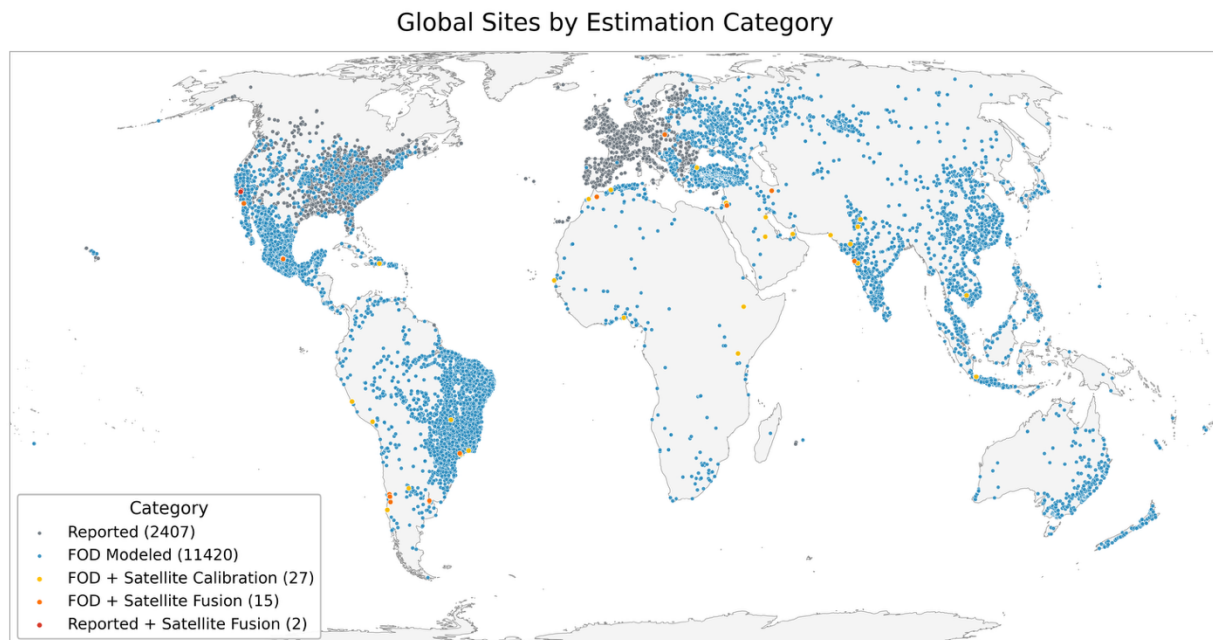


Figure 4. Global Solid Waste Sites by Emission Estimation Methodology Type.

2.2.1 Projection of reported emissions and annual incoming waste (no-FOD pathway)

Where emissions were reported in official government sources like the US EPA, they were assumed to be more accurate than emissions estimated with the FOD pathway due to our lack of comprehensive activity data for many sites. Climate TRACE publishes monthly emissions estimates from 2021-2025, and many landfills either lacked reported emissions for some of the timeframe or the last reported values were dated before the starting year of Climate TRACE data, so in some cases it was desirable to project reported emissions estimates through time. Population-growth-rate based projection was used to fill the gaps.

The equation used for projection was:

$$Q_t = \bar{Q}_R (1 + r)^t,$$

where Q_t is emissions in year t , \bar{Q}_R is the mean of reported emissions, r is a past or future country-level population growth rate, and $t = 0$ is set to the year halfway between the earliest and latest reported emissions years.

After projection, the projected values Q_t were backfilled with $Q_R / 12$ where available.

The same projection and backfilling process was repeated for annual incoming waste values if any were available.

Where landfill closure dates were available, site-specific exponential decay rates k were estimated with the method described in Wang et al. (2024). For sites with emissions reported after the reported closure date, we assumed exponential decay of the waste remaining at the time of closure and re-estimated a new decay rate k by fitting an exponential decay model to the reported post-closure emissions using least-squares. This was justified by our assumption that reported emissions provide a more accurate representation of post-closure landfill behavior than decay rates estimated from waste characteristics and environmental parameters.

2.2.2 Predicting annual incoming waste from the area (FOD pathway)

First-order decay methane emissions models predict, given some input waste, how much of that incoming mass will break down into methane gas and over what time scale. Unfortunately, the source datasets did not contain incoming waste mass values for all SWDS. Where possible, we estimated these values from more widely available landfill surface area data using a hierarchical Bayesian regression model. This framework relates incoming waste to area while accounting for variability across World Bank income groups, which serve as a proxy for differences in waste management intensity and density.

The model was implemented in PyMC and sampled with the No-U-Turn Sampler (NUTS). Model performance was evaluated through leave-one-out cross-validation (LOO-CV), which

showed that the hierarchical model modestly outperformed a simpler linear alternative. Posterior predictive simulations were then used to estimate annual incoming waste for landfills lacking reported values, with credible intervals converted to approximate coefficients of variation to summarize uncertainty.

Full model equations, priors, likelihood structure, validation results, and diagnostic plots are provided in the Supplemental Information (Section SI.2).

2.2.3 SWEET Modeling (FOD pathway)

After running the area-to-incoming-waste model, all sites in the FOD pathway (i.e., those without emissions estimates in source datasets) had associated reported or estimated annual incoming waste values. Methane emissions for these sites were then estimated using the Python implementation of the U.S. EPA SWEET model, created by RMI (RMI, 2025; US EPA, 2025c; https://github.com/RMI/SWEET_python). The SWEET model uses parameters such as incoming waste mass, waste composition, carbon contents, and decay rates to predict a time series of landfill emissions (Table 1). It follows a first-order decay model similar to the standard IPCC first-order decay equation for estimating methane emissions from decaying waste. Parameter values from source datasets were used where available; otherwise, IPCC default values at the country or regional level were applied (IPCC, 2006). Site-specific decay rates were determined with the Wang et al. (2024) model.

Table 1 Parameters used in SWEET python model

I	Month index
j	Waste disposal month
c	Waste component (food, wood, etc)
$L_{\theta,c}$	Methane potential of component c
$k_c(i)$	Decay constant for component c in month i
Δt_i	Month length in years (days in month / days in year)
$MCF(i)$	Methane correction factor in month i
$g(i)$	Gas capture efficiency in month i
$f(i)$	Flare efficiency in month i
$OX(i)$	Oxidation factor in month i

Equation for calculating methane emissions.

$$\text{Let, } S_c(i) = \sum_{u=1}^i k_c(u) \Delta t_u$$

The decay factor $D_c(i,j)$ represents the fraction of waste of component c disposed in month j that remains undecomposed, and contributes to methane generation in a later month $i \geq j$:

$$D_{c(i,j)} = \exp(-\left(S_c(i-1) - S_c(j-1)\right), i \geq j,$$

$$Q_c(i) = \sum_j^i [L_{0,c} w_{j,c} D_{c(i,j)}] (k_c(i) \Delta t_i) MCF(i),$$

$$Q(i) = \sum_c Q_c(i)$$

2.2.4 Incorporating remote sensing measurements

Advances in air- and spaceborne hyperspectral sensors have enabled high-spatial-resolution detection of methane plumes. Prominent data providers include Carbon Mapper and GHGSat, whose instruments combine low detection limits with high spatial resolution, enabling detection and quantification of relatively small plumes. Many of these plumes can be confidently associated with source infrastructure (e.g., O&G pipeline leakages, landfills, animal feeding operations). While the number of landfills being investigated for methane plumes is still orders of magnitude smaller than the total number of landfills on earth, and the temporal frequency of measurements at individual landfills is often low, there are enough satellite measurements at some landfills to meaningfully contribute to waste methane emissions estimation efforts on time scales longer than the instantaneous measurements themselves.

2.2.4.1 Incoming waste calibration for area-modeled sites

The statistical relationship between landfill surface area and annual incoming waste is weak—estimates derived from the area-to-incoming-waste model are highly uncertain (relative uncertainty of 1.5-2.5). Because annual incoming waste is a primary driver of total emissions, inaccuracies in this parameter can lead to substantial errors in modeled results. Although the SWEET model captures the physics and long-term dynamics of landfill processes, its predictive accuracy depends critically on correct annual waste inputs (emissions are an estimated fraction of the total carbon brought into the landfill). Satellite-based methane measurements provide an opportunity to calibrate these inputs to better match observed emissions.

Further details of the optimization framework are provided in Supplemental Information (Section SI.2). Briefly, an initial incoming waste estimate was generated based on the ratio of satellite to FOD model emissions, and the search range was restricted to within a factor of two of this value. A warm-up phase tested a small set of candidate values to locate the best-performing region of the parameter space, after which a focused interval-halving search refined the solution. The procedure terminated when the relative interval width fell below 1% or after a fixed number of iterations.

2.2.4.2 Bayesian scale factor estimation – fusion method

Where annual incoming waste or emissions values were reported, those values were not overwritten with an optimization loop as in Section 2.2.5.1. Instead, we created a Bayesian scale

factor estimation model to combine information from both 1) “bottom-up” reported/FOD-modeled emissions estimates, and 2) “top-down” satellite measurements, into a single predicted emissions time series for a given landfill. This fusion created a posterior predictive time series of landfill emissions.

Specifics of the scale factor fusion model are explained in Supplemental Information SI.3. The final fused emissions time series estimate is $\hat{K}Q_t^{base}$, where Q_t^{base} is the baseline emissions time series predicted by the FOD model and \hat{K} is a scale factor predicted with satellite data and the fusion model.

2.3 Emissions Reduction Solutions (ERS)

Methane mitigation strategies from SWDS generally follow two complementary pathways. The first is midstream waste diversion, which treats organic waste through biological processes such as composting or anaerobic digestion. This approach reduces the quantity of biodegradable material disposed of at SWDS and, consequently, the potential for anaerobic decomposition and methane generation in the long term. The second is downstream improvement of SWDS operations and management, which focuses on enhancing landfill gas (LFG) capture, control, and utilization from waste that is already disposed. The specific mitigation strategies adopted under this pathway, such as installation of a gas collection and control system (GCCS) and destruction of methane through flaring or utilization in an energy project, or oxidation of methane through the use of soil cover or biocover, depend on the engineering and operational characteristics of the site. Importantly, these two pathways are not mutually exclusive; rather, integrated implementation of midstream diversion and downstream gas management has been shown to deliver the greatest overall reduction in methane emissions across the waste sector (Ayandele et al., 2022). Accordingly, the ERS assigned to each SWDS strategy in this analysis represents a compound approach combining both diversion and disposal-site interventions, as detailed in the following sections. *Note: Only rank 1 strategies are provided for assets on the Climate TRACE website and additional strategies will be made available in future releases.*

2.3.1 Waste diversion to composting and anaerobic digestion facilities

An effective way to reduce methane emissions from SWDS is to prevent waste from entering these sites by diverting the waste to composting and anaerobic digestion (AD) facilities. Achievable diversion rate depends on both the timeline and the current and projected future deployment of these technologies. Income level is used as a proxy for both. Each SWDS is assigned an organic waste diversion percentage based on the 2025 [World Bank income classification](#) the country is in, and the diversion percentage ranges from 2% to 18%, with higher income countries expected to be able to treat more waste using composting and AD technologies. See Table 2 for diversion percentage by income group.

Similarly, the split between composting and AD technology deployment differs by income groups. This respective split assigned to each income group is also detailed in Table 2 and assessed through literature review of current and projected composting and AD technology deployment in anchor countries (Kaza et. al., 2018; Babu et al., 2021; Ulloa-Murillo et al., 2022; BMUV, 2023; World Biogas Association, 2019; Kamau & Waswa, 2025; McGaughy et. al., 2024; Pizzanelli et. al., 2023, Jin et. al, 2021). Modeling of induced emissions at composting and AD facilities follows the methodology used in the U.S. EPA's SWEET. Generally, countries in lower income groups divert more waste to composting and less to anaerobic digestion facilities due to the cost and complexities of AD technology and lack of local technical and financial resources.

Table 2: ERS Organic waste diversion rate to composting vs. AD facilities by income group.

World Bank Country Classification by Income	Organic Waste Diversion Rate (% of total waste generated)	Composting / AD split
High Income	17.7%	70% / 30%
Upper Middle Income	12.5%	80% / 20%
Lower Middle Income	12%	90% / 10%
Low Income	1.6%	100% / 0%

2.3.2 Improved methane control at SWDS

Broadly, solid waste disposal sites can be characterized into three types: open dumpsites, controlled dumpsites, and sanitary landfills. Open dumpsites are unmanaged areas where mixed waste is disposed of without liners or cover systems, allowing anaerobic decomposition under uncontrolled conditions that lead to diffuse methane emissions. Controlled dumpsites represent an incremental improvement, with some operational measures such as compaction, limited soil cover, or restricted access, which reduce nuisances but still allow substantial fugitive methane emissions, making retrofitted bio-oxidation or small-scale, basic gas collection systems possible and suitable mitigation strategies to deploy. Sanitary landfills, by contrast, are fully engineered facilities with liners, leachate management, and some also with extensive gas collection to enable systematic methane capture, control, and utilization, significantly reducing overall emissions (Kaza et. al., 2018).

Table 3 shows the ERS assigned to each SWDS type based on site characteristics and available data, as well as the sources each strategy and related assumptions are based on. It is worth noting that in high-income and upper-middle-income countries where the use of regular soil covers on SWDS is generally considered a best practice for methane mitigation, the use of biocover as intermediate cover is recommended as an equivalent strategy. (Disposal Strategies 4&5, 8&9, and 12&13 in Table 3 are three pairs of equivalent strategies for different site types). This approach highlights a technologically proven method to reduce methane emissions potentially significantly by enhancing surface oxidation capacity. Empirical studies have shown that well-maintained biocovers can achieve methane oxidation rates of 30–90%, substantially higher than the 10–20% typically observed in standard soil covers (Scheutz et al., 2017; Abichou et al.,

2009). However, this technology has not yet reached commercial-scale deployment. Its broader adoption in the coming decade will likely depend on enabling factors such as policy incentives, financial mechanisms, and local regulatory support.

Given the availability of more detailed site characteristics and emissions data through GHGRP and LMOP in the United States, the authors have proposed different applicable ERS thresholds for these SWDS aligned with the Maryland Landfill Methane Rule (MDE, 2022). Maryland lowers the applicability threshold to relatively smaller sites (~450,000-ton design capacity) and requires timely installation following defined gas-generation or surface-emission triggers, a more stringent standard than federal rule. This is incorporated to demonstrate emissions reduction potential from sanitary landfills in the U.S. if and when increased ambition is realized through a known, technologically feasible rule. For modeling consistency and clarity, the ERS for sanitary landfills in the U.S. are treated as a separate set of strategies (Disposal Strategy 9-13 in Table 2), although some ERS are similar to those recommended for sanitary landfills in other countries. For a more detailed discussion of the emissions reduction potential of each strategy, see the results section.

Table 3: ERS disposal strategies and corresponding thresholds for applicable threshold for SWDS

Native Strategy id	Applicable SWDS	Strategy Description	Sources
1	Open dumpsites with WIP <250,000 tons	Close these small dumpsites and divert incoming waste to a controlled dumpsite with gas capture and control systems (50% capture efficiency)	IPCC, 2006; IPCC, 2019; U.S. EPA, SWEET User Manual (2025)
2	Open dumpsites with WIP \geq 250,000 tons	Upgrade these sites to controlled dumpsites by adding normal soil cover and gas capture systems (50% capture efficiency)	IPCC, 2019; CDM ACM0001; U.S. EPA, SWEET (2025)
3	Controlled dumpsites currently accepting waste that started to accept waste after 2015 or is located in regions with annual precipitation \leq 1,500 mm	Improve cover practices using normal soil cover at these controlled dumpsite through early application / more frequent inspection for cover integrity etc. to increase oxidation rate to 15%.	IPCC, 2006; IPCC, 2019; U.S. EPA, SWEET User Manual (2025)
4	Controlled dumpsites currently accepting waste in high-income or upper-middle income countries that started to accept waste after 2015 or is located in regions with annual precipitation \leq 1,500 mm	Use biocover as intermediate cover at these controlled dumpsite to increase oxidation rate to 50%	Abichou et al., 2009; Scheutz et al., 2017
5	Controlled dumpsites currently accepting waste that started to accept waste in or before 2015 and is located in regions with annual precipitation $>$ 1,500 mm	Add GCCS with a capture efficiency of 50% to these controlled dumpsites	IPCC 2019, CDM ACM0001; U.S. EPA, SWEET (2025)
6	Non-US sanitary landfills without a GCCS in place but the landfill started accepting waste before	Add GCCS with a capturing efficiency of 50% to the sanitary landfill to capture LFG for flaring or beneficial use	IPCC 2019, CDM ACM0001; U.S. EPA, SWEET (2025)

Native Strategy id	Applicable SWDS	Strategy Description	Sources
7	2015 and is located in a region that with annual precipitation > 1,500 mm Non-US sanitary landfills with an active GCCS in place	Improve the current GCCS capturing efficiency to 60% and flaring efficiency to 90%	IPCC 2019, CDM ACM0001; U.S. EPA, SWEET (2025)
8	Non-US sanitary landfills currently accepting waste that started to accept waste after 2015 or is located in regions with annual precipitation ≤ 1,500 mm Sanitary landfills currently accepting waste in high-income or upper-middle income countries (not the US) that started to accept waste after 2015 or are located in regions with annual precipitation ≤ 1,500 mm	Improve cover practices using normal soil cover at these landfills through early application / more frequent inspection for cover integrity etc. to increase oxidation rate to 15%	IPCC 2019, CDM ACM0001; U.S. EPA, SWEET (2025)
9		Use biocover as intermediate cover at these landfills to increase oxidation rate to 50%	Abichou et al., 2015; Scheutz et al., 2017
10	US sanitary landfills that aren't currently installed with GCCS but will trigger the Maryland Rule Threshold for GCCS installation	Add GCCS with a capturing efficiency of 60% to the sanitary landfill (after incremental increase) to capture LFG for flaring or beneficial use	U.S. EPA, NSPS / Emission Guidelines (40 CFR Part 60); Maryland Rule COMAR 26.11.42 (2023)
11	US sanitary landfills installed with a GCCS with a capturing efficiency or flaring efficiency lower than indicated	Improve the capturing efficiency of current GCCS to 75% and flaring efficiency to 98%	U.S. EPA, NSPS / Emission Guidelines (40 CFR Part 60); Maryland Rule COMAR 26.11.42 (2023)
12	US sanitary landfills that don't have a GCCS in place and wouldn't trigger the installation threshold of the Maryland rule	Improve cover practices using normal soil cover at these landfills through early application / more frequent inspection for cover integrity etc. to increase oxidation rate to 15%	U.S. EPA, NSPS / Emission Guidelines (40 CFR Part 60); Maryland Rule COMAR 26.11.42 (2023), IPCC 2019
13	US sanitary landfills that don't have a GCCS in place and wouldn't trigger the installation threshold of the Maryland rule	Use biocover as intermediate cover at these landfills to increase oxidation rate to 50%	Abichou et al., 2015; Pehme et al., 2020; S. EPA, "Apply Biofilters or Biocovers" guidance

3. Result Highlights and Discussion

This section highlights the results of the site- and country-level methane emissions estimates in the Climate TRACE solid waste dataset and summarizes the mitigation potential of the recommended ERS. It offers key findings on how tailored ERS can inform data-driven mitigation strategies for SWDS worldwide.

3.1 Site-level emissions estimates

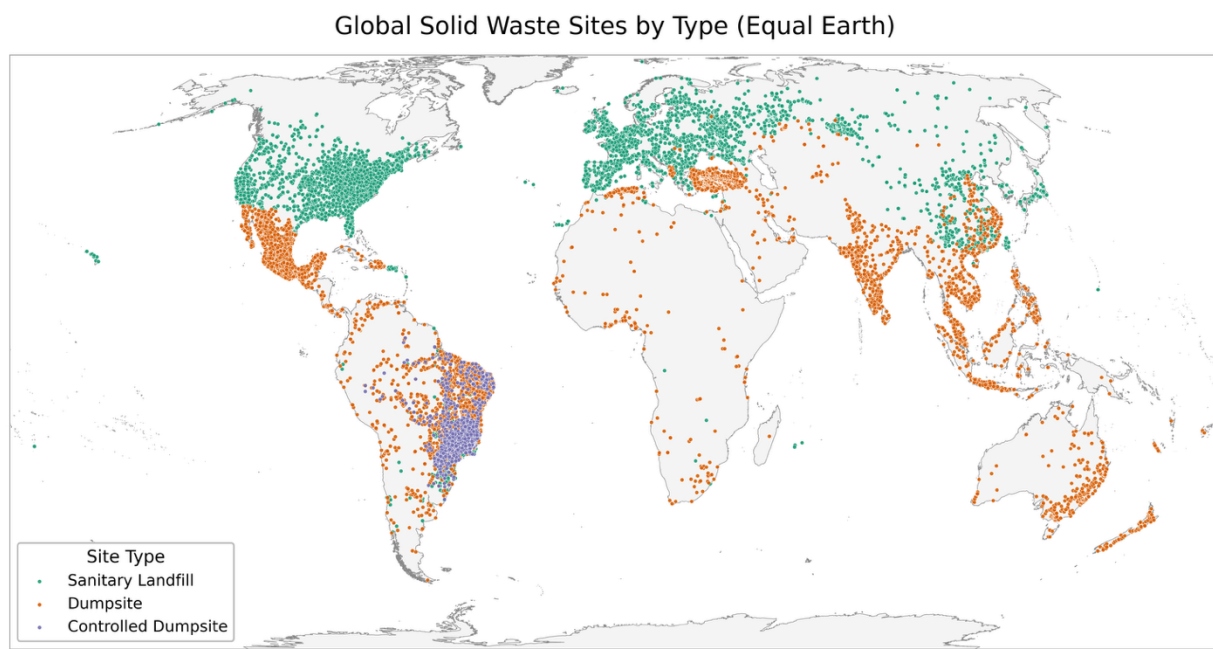


Figure 5 Global Solid Waste Sites by Type: green dots = sanitary landfill, orange dots = dumpsites, and purple dots = controlled dumpsite.

The Climate TRACE global landfill dataset comprises methane emissions estimates for 13,287 solid-waste disposal sites spanning 148 countries. Of these, 11,420 sites (86 %) were generated with the first-order decay (FOD) modelling pathway, while 2,407 were generated with the population-based-projection no-FOD approach. A subset of 44 sites had independent methane measurements from airborne or satellite observations in at least five months; new incoming waste mass estimates were generated for 27 of these sites with the waste mass calibration approach, while the scale factor fusion method was used to generate a new composite methane emissions time series for the remaining 17 sites. All 27 of the waste mass calibration sites were FOD pathway landfills, as were 15 of the 17 sites estimated using the scale factor fusion approach; 2 no-FOD pathway sites had enough available satellite data to qualify for scale factor fusion adjustment. The FOD pathway utilizes the US EPA SWEET methane model, which follows the IPCC 2006 guidelines, estimating methane emissions with decay constants, degradable organic carbon, waste composition, and landfill characteristics such as oxidation rates and gas capture and control systems. Previous research indicates that satellite-based calibration improves emission estimates: top-down remote-sensing studies have found that aerially measured emission rates from US landfills are typically 1.4–2.7 times higher than bottom-up inventory reports (Cusworth et al., 2024).

Across all sites, the average methane emission rate was approximately 1107 t CH₄ yr⁻¹ in 2024 with an average relative uncertainty of about 1 (dimensionless, representing the ratio of the 1 σ standard deviation to the mean). High uncertainty is expected, as the quality and quantity of

available data for most global landfills are low. When expressed as CO₂ equivalent, the mean annual emission is 29909 t CO_{2e} yr⁻¹ (100year GWP) and 88288 t CO_{2e} yr⁻¹ (20year GWP). The surface area of sites averaged 214,177 m², and their biodegradable waste in place averaged 723,943 t. The emission intensity, defined as the tons of methane emitted per ton of biodegradable waste in place, averaged 0.00153 t CH₄ t⁻¹.

No-FOD estimates carried lower uncertainty (~0.3), because that method involves only minor additional adjustments to reasonably high-quality estimates reported by site operators, generally in the United States or the EU. FOD estimates carried a higher uncertainty (~1.2) due to a combination of uncertainty in input data, local environmental data, use of country-level or regional defaults to fill missing input values, and the modeling process itself. Among FOD sites, those calibrated with satellite measurements (optimized waste mass or scale factor methods) exhibited smaller uncertainties (~0.6) because plume-derived emission rates constrain model parameters, and because the plume measurements themselves had lower uncertainty than FOD results. However, because only 42 of 11,420 sites had such data, the overall uncertainty remained dominated by uncalibrated sites. Future expansion of satellite or airborne monitoring will be essential for refining methane inventories and improving confidence in emission intensities and factors.

When satellite plume measurements were used to improve initial emissions estimates, the adjustments tended to be large. The average scale factor \hat{K} from the scale factor fusion pathway was 2.2, meaning, for the 17 sites that qualified for that analytical strategy, the inclusion of satellite data in modeling increased our emissions estimates by 2.2 times. Figures 5 and 6 illustrate two examples of how scale factors influence methane emission time series, along with the corresponding satellite data used for calibration. Figure 6 shows Environmental Complex Norte III, a large landfill in Buenos Aires often featured in waste methane discussions.

Annual incoming waste values calibrated with satellite plume data showed even more pronounced adjustments. The median updated incoming waste values were ~5.3 times larger than the earlier estimates from the area-to-incoming-waste model. Figure 7 shows an FOD time series before and after the waste mass was re-estimated, along with associated satellite data.

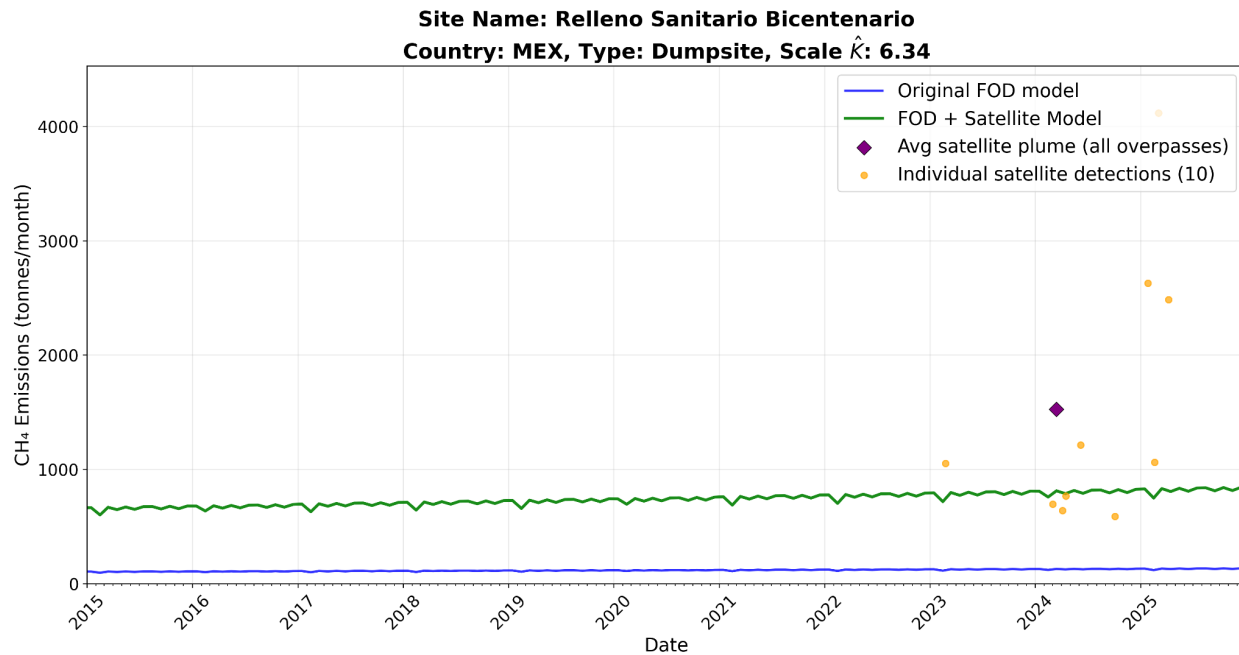


Figure 6. Fusion of satellite observations and modeled data for Relleno Sanitario Bicentenario in Mexico. The green curve represents the final fused emission estimates, integrating modeling results (blue curve) and satellite-based observations (yellow dots).

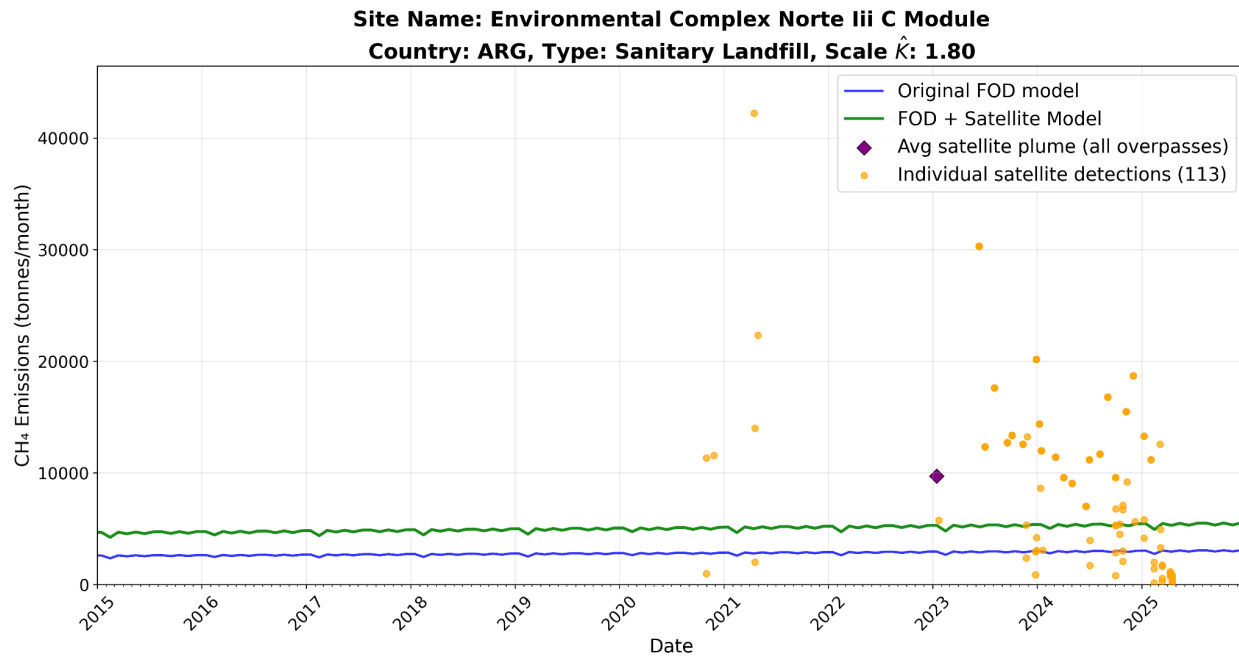


Figure 7. Fusion of satellite observations and modeled data for Environmental Complex Norte iii in Argentina. The green curve represents the final fused emission estimates, integrating modeling results (blue curve) and satellite-based observations (yellow dots).

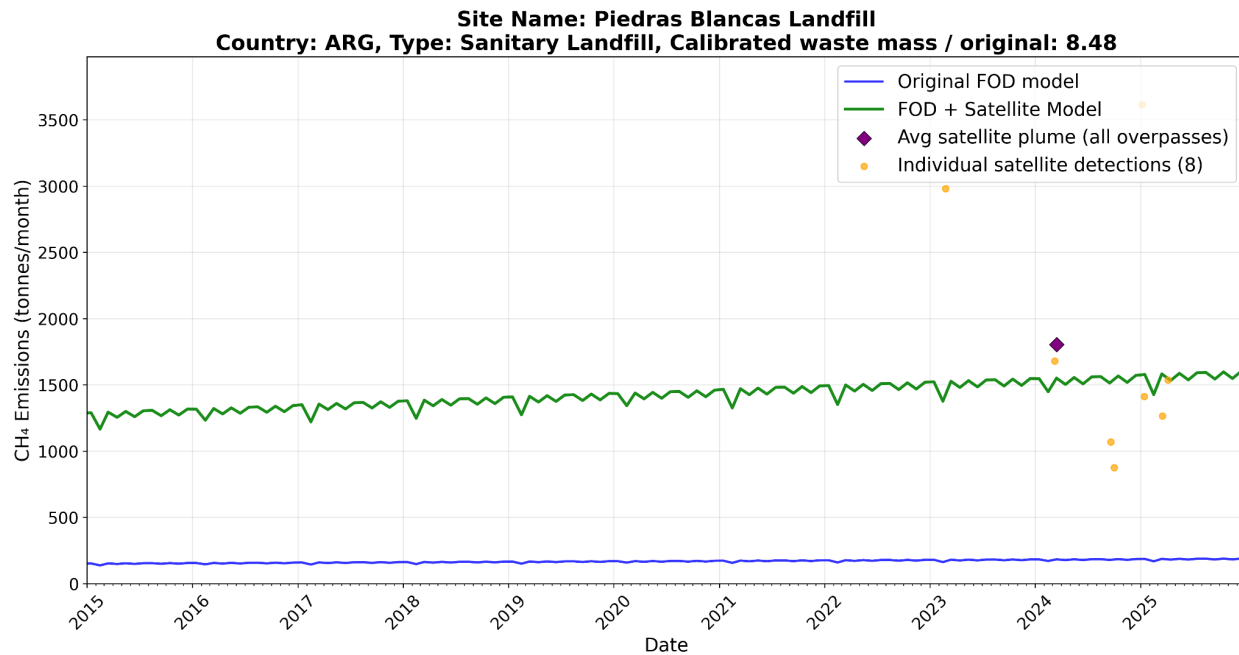


Figure 8. Emission time series estimated from the calibration method for Piedras Blancas Landfill in Argentina. The green curve represents the final emission estimates, calculated using the FOD model with incoming waste amounts calibrated by satellite-based observations. Calibrated waste mass / original gives the ratio of the calibrated waste mass value used to make the green line divided by the original value used for the blue line.

3.2 Country-level emissions estimates

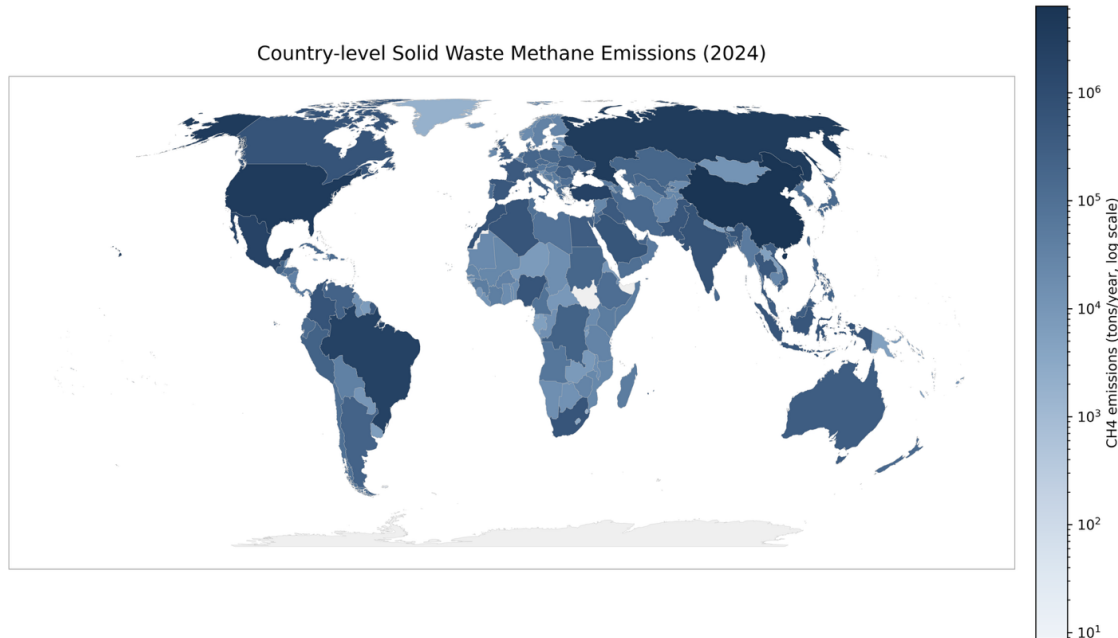


Figure 9 Map of country-level methane emissions.

The country-level dataset includes methane emissions estimates for 211 countries and territories from 2015 to 2025, 148 of which were aggregated from asset-level data. EDGAR projections were used for 63 more. The full Climate TRACE dataset includes 252 countries, but EDGAR or sites data was only available for 211, so 41 countries have unknown emissions. The mean annual methane emission was 187,082 t CH₄ yr⁻¹, while the median value was 26,500 t CH₄ yr⁻¹.

For years and countries where both EDGAR and asset-aggregated estimates existed, EDGAR was the larger value about 86% of the time, with a median factor of 6.4. For the remaining 14%, asset totals were larger than EDGAR by a median factor of 1.8. The countries where EDGAR most exceeded our asset totals were Singapore, Israel, and Burkina Faso; large differences tended to occur in small countries outside the traditional West. Climate TRACE estimates tended to be closer to EDGAR for larger, wealthier countries: EDGAR only exceeded our asset total for the USA by an average of 1.04, for Great Britain by 1.18, and for South Korea by 1.22, and in all those countries our site totals exceeded EDGAR in some years. Other large, wealthy countries were somewhere between those two extremes; EDGAR exceeded our asset totals in France and China by factors of 4.3-4.5, for example. These results are expected: our facilities database is large and growing, but far from comprehensive, especially in less wealthy countries, and EDGAR uses a different methodology. As additional facilities and remote sensing measurements are added, we expect the gap with EDGAR to narrow over time.

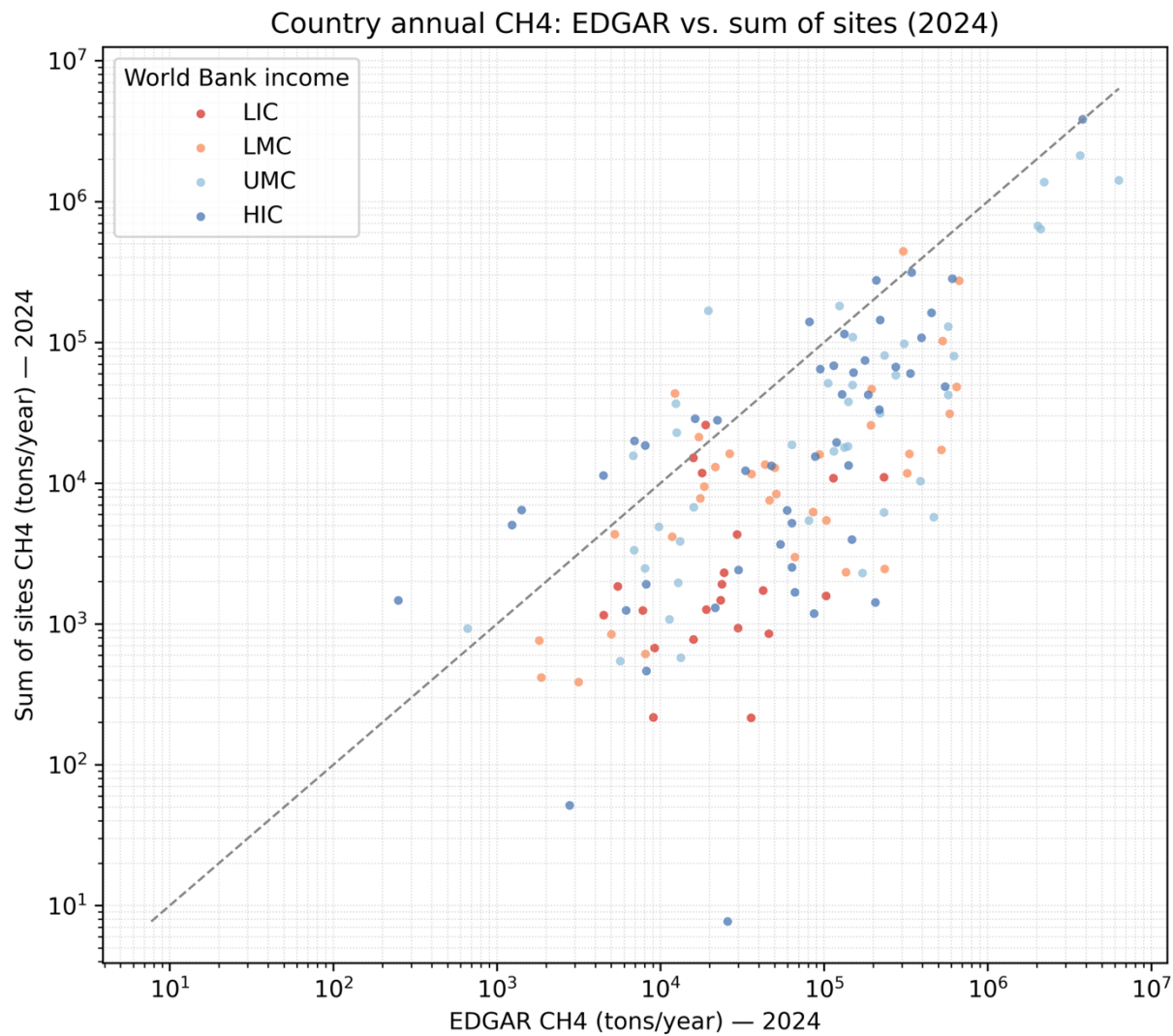


Figure 10. Country-level methane emissions estimates generated by aggregating Climate TRACE assets compared against EDGAR estimates. Each country dot is labeled as HIC = High Income Country (dark blue dots); UMC = Upper Middle Income Country (light blue dots); LMC = Lower Middle Income Country (orange dots); LIC = Low Income Country (red dots).

3.3 Emission Reduction Strategy

In the Climate TRACE data release for November 2025, we recommended an ERS for each SWDS based on available data, including location, income level of the country a given SWDS is in, and other site-specific information, such as GCCS availability, gas collection, and flaring efficiency. Each ERS is a compound strategy combining both diversion and disposal-site interventions. *Note: Only rank 1 strategies are provided for assets on the Climate TRACE website and additional strategies will be made available in future releases.*

Table 4 summarizes the number and criteria of eligible sites for each strategy, along with the corresponding estimated methane mitigation potential. Some sites have more than one recommended strategy, particularly among the three sets of equivalent cover strategies described in Section 2.3.2. Of the 13,287 SWDS, 1,431 are not currently accepting waste, and thus weren't assigned an ERS. For the remaining 11,856 sites, about half are open dumpsites that were assigned a disposal improvement strategy to either close and route incoming waste to a larger, regional site for better environmental control or convert the open dumpsite to a controlled dumpsite through the use of covers and basic GCCS. These two ERS (Strategies #1 and #2) could cut methane emissions from these sites by 20%-30%, assuming that the gas collection efficiency can reach 50%.

For SWDS identified as controlled dumpsites, ERS implementation could cut methane emissions by 25%-63%, depending on the ERS chosen. Holding waste diversion percentages the same, the use of biocover would achieve significantly higher methane emissions reduction than the use of normal soil cover due to higher oxidation rates (Strategy # 4 versus #5).

For SWDS identified as sanitary landfills, ERS would cut methane emissions by 25%-83% (Strategy #6-#13). Holding diversion percentages the same, the implementation of GCCS with a high collection efficiency combined with high-efficiency flares for methane destruction would lead to the highest percentage of methane mitigation at sanitary landfills, and this is especially suitable for older sites located in relatively humid weather (e.g. strategy #7 among strategies #6-#9, and strategy #11 among strategies #10-#13). Similar to controlled dumpsites, the use of biocover as intermediate cover would achieve a higher emissions mitigation than the use of normal soil cover (Strategy #8 versus #9 for non-U.S. sanitary landfills, and Strategy # 12 versus #13 for sanitary landfills in the US).

It is worth noting that the ERS is constrained to one compound strategy per site, except for the equivalent strategies pertaining to the use of biocover versus normal soil cover. This simplification has not yet accounted for greater variation in site conditions in reality. For example, larger dumpsites may see the concurrent implementation of multiple strategies at different parts of the same site, depending on specific conditions. Relatedly, the cut points of an ERS recommendation are limited by the availability of site-level information, which has been discussed above. With more site-specific information available, such as gas collection and flaring efficiency at sanitary landfills, cover materials and compaction practices at dumpsites, finer distinctions can be made to determine the suitability of GCCS installation, efficiency improvements, and biocover use, and thus a more accurate estimate of emission reduction potential can also be made.

Finally, each strategy to reduce emissions has not yet accounted for local political will for strategy implementation for both diversion and disposal improvements, or the project economics

for incorporating specific technologies, such as the deployment of biocover. For more locally tailored strategies, see the [WasteMAP site decision support tool \(DST\)](#) that allows users to estimate the emissions mitigation potential using local data and can assist in simulating a greater number of mitigation scenarios for a single site.

Table 4. Summary of mitigation potential from different ERS strategies. Some sites can have more than one strategy applied. Assets employing specific strategies in this table don't necessarily match what is employed on the Climate TRACE website. See Table 3 for more information on each individual ERS strategy.

Native Strategy id	Applicable SWDS	Number of Sites Assigned this ERS	Strategy Description	Methane mitigation w/ implementation
1	Open dumpsites with WIP <250,000 tons	6119	Close these small dumpsites and divert incoming waste to a controlled dumpsite with gas capture and control systems (50% capture efficiency)	23%
2	Open dumpsites with WIP ≥ 250,000 tons	926	Upgrade these sites to controlled dumpsites by adding normal soil cover and gas capture systems (50% capture efficiency)	32%
3	Controlled dumpsites currently accepting waste that started to accept waste in or before 2015 and is located in regions with annual precipitation > 1,500 mm	108	Add GCCS with a capture efficiency of 50% to these controlled dumpsites	63%
4	Controlled dumpsites currently accepting waste that started to accept waste after 2015 or is located in regions with annual precipitation ≤ 1,500 mm	687	Improve cover practices using normal soil cover at these controlled dumpsite through early application / more frequent inspection for cover integrity etc. to increase oxidation rate to 15%.	25%
5	Controlled dumpsites currently accepting waste in high-income or upper-middle income countries that started to accept waste after 2015 or is located in regions with annual precipitation ≤ 1,500 mm	527	Use biocover as intermediate cover at these controlled dumpsite to increase oxidation rate to 50%	58%
6	Non-US sanitary landfills with an active GCCS in place	3	Improve the current GCCS capturing efficiency to 75% and flaring efficiency to 98%	49%
7	Non-US sanitary landfills without a GCCS in place but the landfill started accepting waste before 2015 and is located in a region that with annual precipitation > 1,500 mm	67	Add GCCS with a capturing efficiency of 75% to the sanitary landfill to capture LFG for flaring (98% efficient) or beneficial use	83%

Native Strategy id	Applicable SWDS	Number of Sites Assigned this ERS	Strategy Description	Methane mitigation w/ implementation
8	Non-US sanitary landfills currently accepting waste that started to accept waste after 2015 or is located in regions with annual precipitation $\leq 1,500$ mm	3354	Improve cover practices using normal soil cover at these landfills through early application / more frequent inspection for cover integrity etc. to increase oxidation rate to 15%	26%
9	Sanitary landfills currently accepting waste in high-income or upper-middle income countries (not the US) that started to accept waste after 2015 or is located in regions with annual precipitation $\leq 1,500$ mm	1220	Use biocover as intermediate cover at these landfills to increase oxidation rate to 50%	64%
10	US sanitary landfills installed with a GCCS with a capturing efficiency or flaring efficiency lower than indicated	8	Improve the capturing efficiency of current GCCS to 75% and flaring efficiency to 98%	47%
11	US sanitary landfills that aren't currently installed with GCCS but will trigger the Maryland Rule Threshold for GCCS installation	732	Add GCCS with a capturing efficiency of 75% to the sanitary landfill (after incremental increase) to capture LFG for flaring (98% efficiency) or beneficial use	65%
12	US sanitary landfills that don't have a GCCS in place and wouldn't trigger the installation threshold of the Maryland rule	500	Improve cover practices using normal soil cover at these landfills through early application / more frequent inspection for cover integrity etc. to increase oxidation rate to 15%	36%
13	US sanitary landfills that don't have a GCCS in place and wouldn't trigger the installation threshold of the Maryland rule	500	Use biocover as intermediate cover at these landfills to increase oxidation rate to 50%	61%

4. Conclusion

The approach adopted by Climate TRACE for the 2025 data release represents a pivotal advancement toward building a seamless pipeline—from developing a comprehensive, global-scale inventory of SWDSs to generating interpretable and observation-informed emissions estimates. A key methodological enhancement over last year's version is the integration of the mechanistic first-order decay model (SWEET model), which enables emissions estimation for individual sites where activity data are available. This advancement supports the design of site-specific Emission Reduction Strategies that target the underlying drivers of emissions. The SWEET model also serves as the foundation for WasteMAP's decision-support tools, which facilitate customized, data-driven decision-making using local information (RMI,

2025). In addition to this mechanistic framework, another major improvement in this year’s data pipeline was the incorporation of more site-level point-source methane satellite observations, and a wholesale change in how they are incorporated into analysis. Where sufficient observations exist, these data are used to calibrate the SWEET model or fuse with reported/modeled emissions, improving the overall accuracy of estimates. As satellite coverage expands over time, our estimates will increasingly converge with observed emissions, enhancing both precision and reliability.

The first step toward improving the emissions accounting for solid waste disposal sites is to develop a higher-confidence, global dataset that comprehensively maps all medium to large landfills and dumpsites. This enhancement is critical because the Climate TRACE 2025 inventory currently relies on multiple data sources with varying levels of confidence regarding site classification, with particularly low reliability in OpenStreetMap-derived data. A more robust inventory would require a greater number of accurately identified and independently verified sites.

Beyond improving site coverage and spatial accuracy, incorporating detailed activity data—such as incoming waste quantities, waste composition, and operational characteristics (e.g., whether a site is a sanitary landfill equipped with gas capture or an unmanaged dumpsite)—is essential for driving the mechanistic model. At present, the modeling pipeline infers incoming waste mass primarily from the landfill area, introducing substantial uncertainty. Enhancing this component of the data pipeline would significantly improve emission estimation accuracy.

Finally, it is important to emphasize that the impact of expanded and more accurate emissions estimates and the newly added emission reducing solutions in Climate TRACE’s data release goes far beyond greenhouse gas emissions mitigation. Solid waste disposal sites, especially open dumpsites common in developing countries, can pose complex environmental and social risks. Communities often live adjacent to or even within these sites, where they are exposed to methane and other harmful gases, pathogens, airborne particulates, toxic leachate, and more. The buildup of unmanaged waste can also lead to spontaneous fires, releasing toxic smoke and further endangering nearby residents. Recognizing these intertwined environmental, health, and safety risks underscores the broader importance of strengthening data and management capacity in the waste sector—efforts that can simultaneously advance climate, public health, and community well-being.

Acknowledgments

The authors would like to express their sincere gratitude to Ebun Ayandele from RMI, Dr. Xunchang Fei from Nanyang Technological University, Dr. Tia Scarpelli from Carbon Mapper, Dr. Bram Maasakkers from SRON, Dr. Malika Menoud from IMEO, Krsna Raniga and Dr. Aaron Davitt from WattTime, Kait Siegel and Paula Garcia Holley from CATF, and Paul

Tulloch, for their valuable contributions to data sharing, discussions on methodology, and insights that greatly enhanced this work. Their expertise and collaboration were instrumental in refining the analysis and ensuring the rigor and relevance of the study.

Supplementary Information

Section SI.1: Solid Waste Emissions Metadata

The solid waste emissions dataset reports CH₄, and 20- and 100-year GWP emissions from individual solid waste disposal sites. CO₂ and N₂O are not explicitly modeled or estimated but are republished from facilities where provided.

Site-level emissions estimates were reported for the years 2021-2025. Country-level emissions estimates span 2015-2025 and reflect a combination of the sum of site-level emissions by country and EDGAR data where coverage was lacking. All data is freely available on the Climate TRACE website (<https://climatetrace.org/>). A detailed description of what is available for download is described in Tables S1 and S2.

Table S1 General dataset information for *Estimating CH₄ Emissions from Solid Waste Disposal Sites*

General Description	Definition
Sector definition	<i>Individual landfill and solid waste disposal site emissions</i>
UNFCCC sector equivalent	<i>4.A Solid Waste Disposal</i>
Temporal Coverage	<i>2021-2025 at facility-level, 2015-2025 at country-level</i>
Temporal Resolution	<i>Monthly</i>
Data format(s)	<i>CSV</i>
Coordinate Reference System	<i>EPSG:4326, decimal degrees</i>
Number of site and countries available for download	<i>13,287 solid waste disposal sites, from 148 countries.</i>
Total emissions for 2024	<i>2.056 billion tons of 100 year CO₂-equivalent</i>
Ownership	<i>We used public data and research to identify ownership information</i>
What emission factors were used?	<i>Model-based emissions factors, motivated by IPCC's first-order decay method from updated 2019 guidelines</i>
What is the difference between a “NULL / none / nan” versus “0” data field?	<i>“0” values are for true non-existent emissions. If we know that the sector has emissions for that specific gas, but the gas was not modeled, this is represented by “NULL/none/nan”</i>

General Description	Definition
total_CO2e_100yrGWP and total_CO2e_20yrGWP conversions	<i>20 year GWP: 79.7</i> <i>100 year GWP: 29.8</i>

Table S2 Facility level metadata description confidence and uncertainty for *Estimating CH₄ Emissions from Solid Waste Disposal Sites*

Data attribute	Confidence Definition	Uncertainty Definition
type	<ul style="list-style-type: none"> <i>Low</i>: Sites labeled dumpsites, from the Global Plastic Watch, as these types are unconfirmed <i>High</i>: Sanitary landfills, if from EPA, Canada, E-PRTR, or Waste Atlas (where type reported) sources 	Not used; N/A
capacity_description	<ul style="list-style-type: none"> <i>Low</i>: OpenStreetMap areas, or where capacities were actively rescaled <i>Medium</i>: Waste Atlas sites, out of date data <i>Very High</i>: Values from EPA sources (self-reported) or Global Plastic Watch (satellite measured) 	+/- 10% from reported values
capacity_factor_description	Not used; N/A	Not used; N/A
capacity_factor_units	Not used; N/A	Not used; N/A
activity	<ul style="list-style-type: none"> <i>Very Low</i>: Modeled values for OpenStreetMap <i>Low</i>: Modeled values for sources other than OpenStreetMap <i>Medium</i>: Self-reported values scaled through 2024 from any source <i>High</i>: Self-reported, unscaled values from Waste Atlas <i>Very High</i>: Self-reported, unscaled values not from Waste Atlas 	<ul style="list-style-type: none"> +/- 10% from reported values 89% confidence interval upper and lower bounds where modeled
CO2_emissions_factor	Not used; N/A	Not used; N/A
CH4_emissions_factor	<ul style="list-style-type: none"> <i>Very Low</i>: Modeled values for OpenStreetMap <i>Low</i>: Modeled values for sources other than OpenStreetMap 	<ul style="list-style-type: none"> +/- 10% from reported values 89% confidence interval upper and

Data attribute	Confidence Definition	Uncertainty Definition
	<ul style="list-style-type: none"> • <i>Medium</i>: LMOP data where gas generated and gas collected both reported • <i>High</i>: All direct self-reported emissions data 	lower bounds where modeled
N2O_emissions_factor	Not used; N/A	Not used; N/A
other_gas_emissions_factor	Not used; N/A	Not used; N/A
CO2_emissions	<ul style="list-style-type: none"> • <i>High</i>: Self-reported emissions values where available 	<ul style="list-style-type: none"> • +/- 10% from reported values
CH4_emissions	Constructed as a weighted combination of activity and emissions factor confidences, quantifying those by scoring from 1-5 as: 1 = very low, 2 = low, 3 = medium, 4 = high, 5 = very high	<ul style="list-style-type: none"> • +/- 10% from reported values • 89% confidence interval upper and lower bounds where modeled
N2O_emissions	<i>High</i> : Self-reported emissions values where available	<ul style="list-style-type: none"> • +/- 10% from reported values
other_gas_emissions	Not used; N/A	Not used; N/A
total_CO2e_100yrGWP	Same as CH4_emissions	<ul style="list-style-type: none"> • +/- 10% from reported values • 89% confidence interval upper and lower bounds where modeled
total_CO2e_20yrGWP	Same as CH4_emissions	<ul style="list-style-type: none"> • +/- 10% from reported values • 89% confidence interval upper and lower bounds where modeled

Table S3 contains descriptions of the column headings found in Climate TRACE ERS strategy data files. Tables S4-16 contain example rows for each of the 13 solid waste sector ERS strategies. More details concerning selecting and ranking strategies can be found in section 3.3 and Table 4.

Table S3 An overview of the ERS schema and column heading descriptions. *Note: Only rank 1 strategies are provided for assets on the Climate TRACE website and additional strategies will be made available in future releases.*

Column Heading	Description
strategy_id	A unique ID for each asset+strategy combination. E.g., rmi_7596_9. Here 7596 is the asset_identifier, and 9 is the strategy reference number.
strategy_name	A descriptive name of the mitigation strategy. E.g., diversion_sanitary_biocover
strategy_description	A short description of the ERS strategy.
mechanism	The mechanism by which the strategy will reduce emissions. It can be one of the following: - 'subtract' : Turning off some or all activity at an asset - 'retrofit' : Changing the technology type or practices of an existing asset
asset_type_new	The new asset type, if the strategy involves converting an asset to a new type.
ch4_emissions_factor_new_to_old_ratio	The ratio of the emissions factor in a scenario where the strategy is applied to a baseline over where the strategy is not applied, e.g., 0.77

Table S4 ERS table example for strategy 1.

Column Heading	Description
strategy_id	rmi_7596_1
strategy_name	diversion_sanitary_biocover
strategy_description	sanitary landfills: add biocover, diversion
mechanism	retrofit
asset_type_new	NA
ch4_emissions_factor_new_to_old_ratio	0.77

Table S5 ERS table example for strategy 2.

Column Heading	Description
strategy_id	rmi_5643_2
strategy_name	diversion_convert_cdump_nobiocover
strategy_description	larger dumpsites: convert to controlled dump, gccs, diversion, no biocover
mechanism	retrofit
asset_type_new	Controlled Dumpsite

Column Heading	Description
ch4_emissions_factor_new_to_old_ratio	0.68

Table S6 ERS table example for strategy 3.

Column Heading	Description
strategy_id	rmi_9884_3
strategy_name	diversion_cdump_add_gccs
strategy_description	controlled dumpsites: add GCCS (gas collection), diversion
mechanism	retrofit
asset_type_new	NA
ch4_emissions_factor_new_to_old_ratio	0.37

Table S7 ERS table example for strategy 4.

Column Heading	Description
strategy_id	rmi_10327_4
strategy_name	diversion_cdump_nobiocover
strategy_description	controlled dumpsites: no biocover, diversion
mechanism	retrofit
asset_type_new	NA
ch4_emissions_factor_new_to_old_ratio	0.75

Table S8 ERS table example for strategy 5.

Column Heading	Description
strategy_id	rmi_3257_5
strategy_name	diversion_cdump_biocover
strategy_description	controlled dumpsites: add biocover, diversion
mechanism	retrofit
asset_type_new	NA
ch4_emissions_factor_new_to_old_ratio	0.42

Table S9 ERS table example for strategy 6.

Column Heading	Description
strategy_id	rmi_6061_6
strategy_name	diversion_sanitary_improve_gccs
strategy_description	sanitary landfills: improve existing GCCS, diversion
mechanism	retrofit
asset_type_new	NA
ch4_emissions_factor_new_to_old_ratio	0.51

Table S10 ERS table example for strategy 7.

Column Heading	Description
strategy_id	rmi_12223_7
strategy_name	diversion_sanitary_add_gccs
strategy_description	sanitary landfills: improve existing GCCS, diversion sanitary landfills: add GCCS, diversion
mechanism	retrofit
asset_type_new	NA
ch4_emissions_factor_new_to_old_ratio	0.17

Table S11 ERS table example for strategy 8.

Column Heading	Description
strategy_id	rmi_4453_8
strategy_name	diversion_sanitary_add_gccs
strategy_description	sanitary landfills: no biocover, diversion
mechanism	retrofit
asset_type_new	NA
ch4_emissions_factor_new_to_old_ratio	0.74

Table S12 ERS table example for strategy 9.

Column Heading	Description
strategy_id	rmi_5764_9
strategy_name	diversion_sanitary_biocover

Column Heading	Description
strategy_description	sanitary landfills: add biocover, diversion
mechanism	retrofit
asset_type_new	NA
ch4_emissions_factor_new_to_old_ratio	0.36

Table S13 ERS table example for strategy 10.

Column Heading	Description
strategy_id	rmi_1633_10
strategy_name	diversion_us_sanitary_improve_gccs
strategy_description	US sanitary landfills: improve GCCS, diversion
mechanism	retrofit
asset_type_new	NA
ch4_emissions_factor_new_to_old_ratio	0.53

Table S14 ERS table example for strategy 11.

Column Heading	Description
strategy_id	rmi_10776_11
strategy_name	strategy11_us_sanitary_add_gccs
strategy_description	US sanitary landfills: add GCCS, diversion
mechanism	retrofit
asset_type_new	NA
ch4_emissions_factor_new_to_old_ratio	0.35

Table S15 ERS table example for strategy 12.

Column Heading	Description
strategy_id	rmi_9922_12
strategy_name	strategy12_us_sanitary_nobiocover
strategy_description	US sanitary landfills: no biocover, diversion
mechanism	retrofit
asset_type_new	NA

Column Heading	Description
ch4_emissions_factor_new_to_old_ratio	0.64

Table S16 ERS table example for strategy 13.

Column Heading	Description
strategy_id	rmi_5431_13
strategy_name	strategy13_us_sanitary_biocover
strategy_description	US sanitary landfills: add biocover, diversion
mechanism	retrofit
asset_type_new	NA
ch4_emissions_factor_new_to_old_ratio	0.39

Permissions and Use: All Climate TRACE data is freely available under the Creative Commons Attribution 4.0 International Public License, unless otherwise noted below.

Data citation format: Runyan, H., Wu, Y., Scheinwald, A., Wang, Y., Frankiewicz, T., McGrath, J. & Raniga, K. (2025). *Solid Waste Sector- Estimating CH4 Emissions from Solid Waste Disposal Sites*. WattTime, USA, Climate TRACE Emissions Inventory. <https://climatetrace.org> [Accessed date]

Geographic boundaries and names (iso3_country data attribute): The depiction and use of boundaries, geographic names and related data shown on maps and included in lists, tables, documents, and databases on Climate TRACE are generated from the Global Administrative Areas (GADM) project (Version 4.1 released on 16 July 2022) along with their corresponding ISO3 codes, and with the following adaptations:

- HKG (China, Hong Kong Special Administrative Region) and MAC (China, Macao Special Administrative Region) are reported at GADM level 0 (country/national);
- Kosovo has been assigned the ISO3 code ‘XKX’;
- XCA (Caspian Sea) has been removed from GADM level 0 and the area assigned to countries based on the extent of their territorial waters;
- XAD (Akrotiri and Dhekelia), XCL (Clipperton Island), XPI (Paracel Islands) and XSP (Spratly Islands) are not included in the Climate TRACE dataset;
- ZNC name changed to ‘Turkish Republic of Northern Cyprus’ at GADM level 0;
- The borders between India, Pakistan and China have been assigned to these countries based on GADM codes Z01 to Z09.

The above usage is not warranted to be error free and does not imply the expression of any opinion whatsoever on the part of Climate TRACE Coalition and its partners concerning the legal status of any country, area or territory or of its authorities, or concerning the delimitation of its borders.

Disclaimer: The emissions provided for this sector are our current best estimates of emissions, and we are committed to continually increasing the accuracy of the models on all levels. Please review our [terms of use](#) and the sector-specific [methodology documentation](#) before using the data. If you identify an error or would like to participate in our data validation process, please [contact us](#).

Section SI.2: Area-to-incoming-waste model

Source datasets did not contain annual incoming waste values for all landfills, and landfill surface areas were much more widely available than annual incoming waste. We chose to estimate annual incoming waste from surface area with a hierarchical Bayesian regression framework. Hierarchical (or multilevel) models are designed to handle grouped data, accounting for shared variability within groups and allowing for partial pooling between them. In this case, landfills were nested within World Bank income groups, because landfill waste densities are often contingent on management intensity, and management intensity correlates with country/region income (Kaza et al., 2018).

We assume that the expected incoming waste for a landfill grows proportionally with area. To reflect this proportionality, the model is specified on the logarithmic scale: the logarithm of incoming waste is modeled as an income-group-specific intercept plus an income-group-specific slope multiplying the logarithm of area, with a random intercept for each site. The slopes for the income groups are given log-normal prior distributions, ensuring strictly positive scaling and accommodating the right-skewed nature of waste data. The intercepts are drawn from normal distributions with shared hyper-priors to allow partial pooling across sites. The observational model uses a Student's t likelihood on the log scale, which has heavier tails than a Gaussian distribution and is therefore less sensitive to outliers (Gelman & Hill, 2006; Lange et al., 1989).

Let A_i denote the area of a landfill where i is an index of all combinations of area and annual incoming waste values, Y_i the observed annual incoming waste, g_i the World Bank income-group index, and s_i the landfill index. Each landfill s can have multiple indices denoted by i corresponding to different years.

Slopes and intercepts by income group. Each income group has a log-space slope κ . Define the intercept group-level priors as

$$\mu_\kappa \sim N(1, 0.5),$$

$$\sigma_\kappa \sim HN(0.5),$$

$$\kappa_g \sim (\mu_\kappa, \sigma_\kappa),$$

$$g = 1, \dots, N_{income},$$

where N_{income} is the number of income groups.

Compute an initial estimate β_0 as the median ratio of incoming waste to area in the training data.

Define the intercept group-level priors as

$$\mu_\alpha \sim N(\log \beta_0, 0.5),$$

$$\sigma_\alpha \sim HN(0.5),$$

$$\alpha_g \sim (\mu_\alpha, \sigma_\alpha),$$

$$g = 1, \dots, N_{income},$$

where N_{income} is the number of income groups. The Log-Normal prior restricts α_g to positive values and allows group-specific differences in waste density.

Random Intercepts. To account for persistent site-level deviations, random intercepts were introduced:

$$\alpha_{site[s]} \sim N(0, \tau_{site})$$

$$\tau_{site} \sim HN(0.4)$$

These terms are included for each site s . They preserve the boundary condition that zero area implies zero waste, because the multiplicative factors vanish when $A_i = 0$.

Mean structure. Express the expected incoming waste on the log scale as

$$\log \mu_i = \alpha_g + \kappa_{g_i} \log (A_i + \epsilon) + \alpha_{site[s_i]},$$

where $\epsilon = 10^{-12}$ is a small constant to avoid taking the logarithm of zero. On the original scale, this becomes

$$\mu_i = \exp(\alpha_g) (A_i + \epsilon)^{\kappa_{g_i}} \exp(\alpha_{site[s_i]})$$

Likelihood. Model the observations with a Student's t distribution on the log scale:

$$\nu \sim Exponential\left(\frac{1}{10}\right) + 2$$

$$\sigma \sim HN(0.3)$$

$$\log Y_i \sim StudentT(\nu, \log \mu_i, \sigma)$$

The heavytailed Student's t distribution reduces the influence of outliers.

Capping of predictions. To avoid unrealistic estimates caused by very large areas or long-tailed distributions, the predicted mean annual incoming waste was capped at 500,000 t yr⁻¹, with a lower bound set at 10⁻¹⁰ t yr⁻¹, reflecting practical limits on waste generation.

The model is implemented in PyMC (Abril-Pla et al., 2023) and sampled with the No-U-Turn Sampler (Hoffman & Gelman, 2014), an adaptive Hamiltonian Monte Carlo variant that is widely used as a default for general-purpose Bayesian inference. Posterior distributions for the parameters were obtained via Markov chain Monte Carlo sampling. Posterior predictive simulations were then used to estimate incoming waste for landfills with known area but missing incoming waste data. For each landfill, we calculated the posterior predictive median along with 89% credible intervals (central highest density intervals). To summarize uncertainty as a single metric, we converted these bounds to an approximate one-sigma coefficient of variation (relative uncertainty) under a log-normal approximation to the posterior predictive distribution (Limpert et al., 2001; Proost, 2019).

Leave-one-out cross-validation (LOO-CV) was used to estimate out-of-sample predictive fit in PyMC, as a means of model comparison. This process systematically omits one data point at a time, trains on the remaining data, evaluates the log-likelihood of the omitted point, and aggregates these values into final scores (McElreath, 2018). In Table 1 below, a less negative “elpd_loo” (expected log pointwise predictive density) is preferable. “p_loo” represents the effective number of parameters, capturing model complexity. “se” is the standard error of the “elpd_loo” calculation. “rank” is a synthesis of these variables, running from the most to least preferred model (0 is most preferable).

Table S3 shows model performance metrics for the hierarchical model we used, and a simpler one (Basic Linear) that did not include separate income categories. Table S18 does not indicate drastic differences between the two model structures, though the “Basic Linear” model performs worse.

Table S18 LOO cross-validation comparison results for Model 1 (emissions model).

	rank	elpd_loo	p_loo	weight	se
Hierarchical	0	-3054.49	3561.98	0.62	214.99
Basic Linear	1	-23267.67	8.777807	8.780.38	153.82

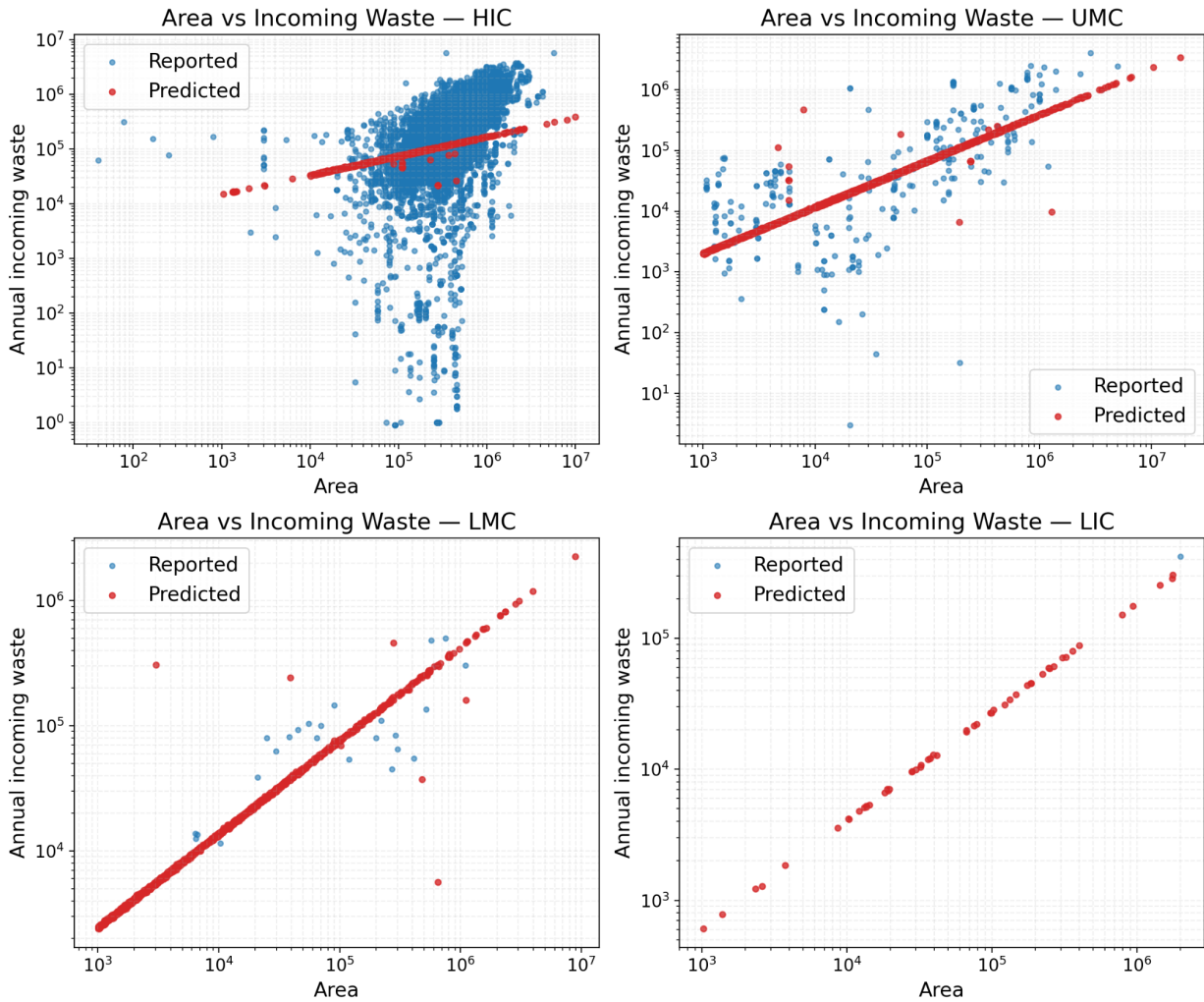


Figure S1: Plots of area vs incoming waste showing reported values and predictions from the area-to-incoming-waste model. a) High income countries, b) Upper middle income, c) Lower middle income, d) Lower income.

Section SI.3: Incoming waste calibration

To improve estimates of annual incoming waste, a dichotomous (interval-halving) search optimization was applied to minimize the error between modeled and satellite-observed methane emissions. The algorithm iteratively predicts a new annual incoming waste value, projects backward and forward in time with country-level population growth rates, and evaluates the error between a SWEET-predicted time series and available satellite data for that landfill. Then, a new annual incoming waste value is chosen with the interval-halving search method, and then the process is repeated until a minimum error value is reached. Because the relationship between waste mass and predicted emissions is monotonic, a one-dimensional search algorithm can efficiently find the incoming waste amount that minimizes the error.

Let M denote the annual incoming waste mass (t yr^{-1}). For each candidate M , the SWEET model generates a time series of predicted methane emission rates, $Q_t^{\text{base}}(M)$ for each month t from the site-specific- start year to the end year. Let Q_t^{sat} denote the corresponding satellite-derived-emissions at observation months $t \in O$, where O is the set of months with at least one overpass. Monthly satellite observations were obtained by averaging observations within each month. Then, the error between model and observation is quantified using a weighted root-mean-square error objective function.

Optimization Procedure:

1. **Initial guess:** Compute an initial estimate M_0 as the ratio of satellite to model emissions at the site,

$$M_0 = M_{\text{est}} \times \frac{1}{n} \sum_{t=1}^n \frac{Q_t^{\text{sat}}}{Q_t^{\text{base}}(M_{\text{est}})} ,$$

where n is the site-specific number of months in O , and M_{est} is the uncertain incoming waste mass value estimated with the area-to-incoming-waste model. Restrict the search range to a factor of two around this guess, $[M_0/2, 2M_0]$.

2. **Warm-up tests:** Evaluate the objective function at M_0 and at a few points around it ($0.5\times$, $0.75\times$, $1.25\times$ and $1.5\times$ the initial guess). Select the mass with the smallest error.
3. **Focused dichotomous (interval-halving) search:** Center a narrow interval ($\pm 20\%$) around the best candidate and perform an interval-halving search. At each iteration, evaluate the objective function at the midpoint M^* and evaluate the error. If the error improves upon the current best, update the best mass and narrow the interval. The search terminates when the relative width of the interval falls below 1 % or after a fixed maximum number of evaluations (e.g., 20). The optimized waste mass is $\hat{M} = M^*$, with the associated minimum error recorded as err_{\min} (Nocedal & Wright, 2006).

Uncertainty estimation: Delta-method uncertainty propagation. While it would be preferable to quantify uncertainty in the estimation of optimum incoming waste \hat{M} and the resulting emissions through direct resampling (e.g., bootstrapping), the SWEET model is too computationally expensive for that to be practical. We used a delta method approximation instead, which linearizes a differentiable transformation and propagates uncertainty via the derivative (Oehlert, 1992; van der Vaart, 1998). The delta method linearizes a nonlinear function around the optimum and uses derivatives to propagate errors through the function. More formally, if a nonlinear transformation $G(X)$ is differentiable, the standard error of $G(X)$ can be approximated by the first derivative and the standard error of X :

$$\sigma_{G(X)} \approx |G'(X)|\sigma_x$$

This approach approximates the local behavior of a non-linear function by its tangent line near the point of interest.

Applying the delta method to our application, for each month the variance of the log emissions due to uncertainty in θ is approximated by

$$Var(\log Q_t) \approx S_t^2 Var(\theta)$$

$$S_t = \frac{\partial \log Q_t}{\partial \theta}$$

To solve for the variance of predicted monthly emissions estimates, it is necessary to calculate the right hand part of this equation, starting with elasticity S_t .

Uncertainty estimation: Sensitivity analysis. Define $\theta = \log(M)$ and let $\hat{M} = \exp(\theta_0)$ be the optimal incoming waste mass. The SWEET model is run three times:

- 1) at the optimum mass, giving baseline series $\hat{Q}_t(\hat{M})$;
- 2) at an increased mass $\hat{M}\exp(\epsilon)$; and
- 3) at a decreased mass $\hat{M}\exp(-\epsilon)$,

where ϵ is a small perturbation (e.g., 0.01). The elasticity of each month's predicted emission with respect to θ is estimated by a central difference on the log scale:

$$S_t = \frac{\partial \log Q_t(\theta)}{\partial \theta}$$

$$S_t \approx \frac{\log \hat{Q}_t(\hat{M}\exp(\epsilon)) - \log \hat{Q}_t(\hat{M}\exp(-\epsilon))}{2\epsilon}$$

At the observation months $t \in O$ the derivative J_i between log emissions and θ is computed similarly. These derivatives quantify how sensitive each predicted emission is to changes in θ (Saltelli et al., 2007).

Uncertainty estimation: Observation-error weighting. The variance of θ is approximated by the reciprocal of the information, $Var(\theta) \approx I(\theta)^{-1}$ (van der Vaart, 1998). Assuming independent observations, the one-dimensional Fisher information is

$$I(\theta) = \sum_i \frac{J_i^2}{\sigma_i^2},$$

where

$$J_i = \frac{\partial \log Q_{t_i}}{\partial \theta},$$

is the sensitivity (slope) of the log-predicted emission at observation month t_i with respect to θ , and σ_i^2 is the variance of the log-emission error at the observation (including satellite and model noise).

Satellite measurements and FOD model predictions each carry an associated uncertainty. Define $CV_{sat,i}$ and $CV_{base,i}$ as the coefficients of variation (relative standard deviation) for individual satellite observations, and $CV_{base,i}$ as the coefficient of variation for individual model predictions. The standard deviation of log emissions for each observation is

$$\sigma_i^2 = \sigma_{sat,i}^2 + \sigma_{base,i}^2,$$

where σ_{sat} and σ_{base} are obtained from the coefficients of variation via $\sigma = \sqrt{\log(1 + CV^2)}$ (JCGM 100:2008, n.d.; Limpert et al., 2001).

With both S_t and $Var(\theta)$ calculated, post-optimization emissions uncertainty for this pathway can be calculated with the original equation.

$$Var(\log \log Q_t) \approx S_t^2 Var(\theta)$$

Uncertainty estimation: Packaging results. The delta-method calculation produces a table of monthly statistics consisting of:

- mean: $\hat{Q}_t(\hat{M})$
- standard deviation: $\hat{Q}_t \times CV_t$
- relative 1- σ : CV_t
- 16th, 50th, and 84th percentiles of the lognormal distribution implied by the mean and coefficient of variation (log-scale +/- 1 σ).

Additionally, the standard deviation σ_θ and the total relative uncertainty CV_{total} were calculated. Because the delta method linearizes the model around the optimum, these uncertainty measures

are approximate and reflect local sensitivity; they do not account for potential non-linearity far from \hat{M} or structural model errors.

Section SI.4: Scale factor fusion

The following paragraphs explain the mathematical arrangement of the Bayesian scale factor fusion model.

Definition of the posterior model.

Let Q_t^{base} denote the baseline model emissions at month t from either the FOD or no-FOD pathway, and y_t be the plume-derived emissions measurement at month t . We seek a multiplicative scale factor K such that the scaled emissions KQ_t^{base} include information from both mechanistic “bottom-up” FOD modeling and also “top-down” satellite measurements (Gelman et al., 2013; Kennedy & O’Hagan, 2001; Poole & Raftery, 2000).

The arrangement of the model is explained in the following paragraphs. Define the parameters $\Theta = (\log K, \log s)$, where $s > 0$ is the standard deviation of the log-space measurement error.

Baseline mean. For each observation month t , the pre-satellite modeled baseline mean on the log scale is

$$\mu_t = \log(K Q_t^{base})$$

We treat emissions as strictly positive. Modeling log emissions as Gaussian ensures positivity of the emissions and yields a lognormal distribution on the original scale.

Priors. We place a gaussian prior

$$\log K \sim N(m_0, s_0^2),$$

with location m_0 and standard deviation s_0 . We model s with a half-normal prior,
 $s \sim HN(\sigma_{prior})$

Meaning the density of s is proportional to a normal density with mean zero and standard deviation σ_{prior} , truncated to $s > 0$.

Likelihood for detections. If y_t is a detected plume, we assume that its logarithm is normally distributed around μ_t with variance $s^2 + v_t$:

$$\log y_t \sim N(\mu_t, s^2 + v_t)$$

Here ν_t is the measurement variance on the log scale,

$$\nu_t = \text{Var}(\log y_t) \approx \log \left(1 + \left(\frac{\text{SE}_t}{y_t} \right)^2 \right),$$

where SE_t is the reported standard error of the plume measurement. The contribution of a detected observation to the negative log-likelihood is

$$l_{\text{detect}}(\Theta) = \frac{1}{2} \frac{(\log y_t - \mu_t)^2}{s_{\text{eff},t}^2} + \log s_{\text{eff},t} + \frac{1}{2} \log 2\pi,$$

with $s_{\text{eff},t}^2 = s^2 + \nu_t$.

Likelihood for non-detections. When a satellite images a landfill but no methane plume is detected, we do not know that emissions were 0; we only know that emissions were below the detection limit L . We treat this as left-censored data from a log-normal distribution (Helsel, 2012). For a non-detection, the likelihood contribution is the log of the cumulative distribution function (CDF):

$$l_{\text{non-detect}}(\Theta) = -\log \Phi(c_t),$$

where

$$c_t = \frac{\log L_t - \mu_t}{s_{\text{eff},t}},$$

and Φ is the standard normal CDF (Amemiya, 1984).

Total negative log posterior. Combining the priors and likelihood contributions across all observation months, the negative log posterior is (prior on $\log K$ is first non-sum term, second is prior on s , can add little brackets to show that if necessary).

$$\begin{aligned} NLP(\Theta) = & \frac{1}{2} \frac{(\log K - m_0)^2}{s_0^2} + \log s_0 + \frac{1}{2} \log 2\pi + \sum_{\text{detections}} [l_{\text{detect}}(\Theta)] + \\ & \sum_{\text{non-detections}} [\Phi(c_t)] + \frac{1}{2} \left(\frac{s}{\sigma_{\text{prior}}} \right)^2 \end{aligned}$$

Maximum a posteriori estimation. We obtain the maximum a posteriori (MAP) estimate $\hat{\Theta} = (\hat{\log K}, \hat{\log s})$ by optimizing the log posterior (Nocedal & Wright, 2006). Let

$$H = \nabla^2 [-\log p(y)] \Big|_{\Theta=\hat{\Theta}}$$

denote the observed information (the Hessian of the negative log posterior) at the MAP. Under the Laplace/normal approximation, the posterior is approximately $N(\hat{\Theta}, H^{-1})$ (Bishop, 2006; Tierney & Kadane, 1986). Thus, the approximate variance of $\log K$ is $\text{Var}(\log K) \approx (H^{-1})_{kk}$ —where k is an index of parameters ($\log K \rightarrow 1$, $\log s \rightarrow 2$) and also the diagonal element at

location(k,k) of inverse Hessian H^{-1} —and $sd(\log K) \approx \sqrt{(H^{-1})_{kk}}$. This aligns with asymptotic likelihood theory, where the inverse observed information gives the covariance (van der Vaart, 1998). Transforming back gives an approximate 95% interval for K by exponentiating the log-scale endpoints:

$$K \in [\exp \exp(\hat{\log K} - 1.96 sd(\log K)), \exp \exp(\hat{\log K} + 1.96 sd(\log K))]$$

The final scaled estimated emissions time series is then calculated with \hat{KQ}_t^{base} .

References

1. 40 CFR Part 60 Subpart WWW -- Standards of Performance for Municipal Solid Waste Landfills That Commenced Construction, Reconstruction, or Modification on or After May 30, 1991, but Before July 18, 2014. (n.d.). Retrieved October 28, 2025, from <https://www.ecfr.gov/current/title-40/part-60/subpart-WWW>
2. Abichou, T., Mahieu, K., Yuan, L., Chanton, J., & Hater, G. (2009). Effects of compost biocovers on gas flow and methane oxidation in a landfill cover. *Waste Management*, 29(5), 1595–1601. <https://doi.org/10.1016/j.wasman.2008.11.007>
3. Abril-Pla, O., Andreani, V., Carroll, C., Dong, L., Fonnesbeck, C. J., Kochurov, M., Kumar, R., Lao, J., Luhmann, C. C., Martin, O. A., Osthege, M., Vieira, R., Wiecki, T., & Zinkov, R. (2023). PyMC: A modern, and comprehensive probabilistic programming framework in Python. *PeerJ Computer Science*, 9, e1516. <https://doi.org/10.7717/peerj-cs.1516>
4. Amemiya, T. (1984). Tobit models: A survey. *Journal of Econometrics*, 24(1), 3–61. [https://doi.org/10.1016/0304-4076\(84\)90074-5](https://doi.org/10.1016/0304-4076(84)90074-5)
5. Ayandele, E., Huffman, K., Jungclaus, M., Tseng, E., Duren, R., Cusworth, D. and Fisher, B., 2022. *Key Strategies for Mitigating Methane Emissions from Municipal Solid Waste*, RMI, <https://rmi.org/insight/mitigating-methane-emissions-from-municipal-solid-waste/> [Accessed 01 September 2022].
6. Babu, R., Prieto Veramendi, P. M., & Rene, E. R. (2021). Strategies for resource recovery from the organic fraction of municipal solid waste. *Case Studies in Chemical and Environmental Engineering*, 3, 100098. <https://doi.org/10.1016/j.cscee.2021.100098>
7. Bishop, C. M. (2006). *Pattern Recognition and Machine Learning*. Springer Science+Business Media, LLC.
8. Safety, F. M. for the E., Nature Conservation, Nuclear, & and Consumer Protection (BMUV). (2023). *Waste Management in Germany 2023 Facts, data, figures*. https://www.bmuv.de/fileadmin/Daten_BMU/Pools/Broschueren/abfallwirtschaft_2023_en_bf.pdf
9. Carbon Mapper, Inc. (2025). *Carbon Mapper* [Dataset]. <https://carbonmapper.org/data> [10/01/2025]

10. Clean Air Task Force (CATF). (2025). *CATF Waste Database* [Dataset]. <https://www.catf.us/> [08/01/2025]
11. Cusworth, D. H., Duren, R. M., Ayasse, A. K., Jiorle, R., Howell, K., Aubrey, A., Green, R. O., Eastwood, M. L., Chapman, J. W., Thorpe, A. K., Heckler, J., Asner, G. P., Smith, M. L., Thoma, E., Krause, M. J., Heins, D., & Thorneloe, S. (2024). Quantifying methane emissions from United States landfills. *Science (New York, N.Y.)*, 383(6690), 1499–1504. <https://doi.org/10.1126/science.adf7735>
12. European Union (2025). *European Pollutant Release and Transfer Register* [Dataset]. <https://industry.eea.europa.eu/> [08/01/2025]
13. Federative Republic of Brazil. (2019). *The Sistema Nacional de Informações sobre a Gestão dos Resíduos Sólidos (SINIR)* [Dataset]. <https://relatorios.sinir.gov.br/relatorios/municipal/> [08/01/2025]
14. Gelman, A., Carlin, J. B., Stern, H. S., Dunson, D. B., Vehtari, A., & Rubin, D. B. (2013). *Home page for the book, “Bayesian Data Analysis”* (3rd ed.). Chapman & Hall (CRC Press). <https://sites.stat.columbia.edu/gelman/book/>
15. Gelman, A., & Hill, J. (2006). *Data Analysis Using Regression and Multilevel/Hierarchical Models*. Cambridge Aspire Website; Cambridge University Press. <https://doi.org/10.1017/CBO9780511790942>
16. GHGSat. (2025). *GHGSat Inc.* <https://www.ghgsat.com/en/>
17. Global Plastic Watch. (2021). *Global Plastic Watch (GPW)* [Dataset]. <https://www.globalplasticwatch.org/> [08/01/2025]
18. Government of Canada. (2025). *Canada Greenhouse Gas Reporting Program (GHGRP)* [Dataset]. <https://www.canada.ca/en/environment-climate-change/services/climate-change/greenhouse-gas-emissions/facility-reporting.html> [08/01/2025]
19. Helsel, D. R. (2012). *Statistics for Censored Environmental Data Using Minitab and R* (2nd ed.). John Wiley & Sons, Inc. <https://www.wiley.com/en-us/Statistics+for+Censored+Environmental+Data+Using+Minitab+and+R%2C+2nd+Edition-p-9780470479889>
20. Hoffman, M. D., & Gelman, A. (2014). The No-U-turn sampler: Adaptively setting path lengths in Hamiltonian Monte Carlo. *J. Mach. Learn. Res.*, 15(1), 1593–1623.
21. IPCC (Intergovernmental Panel on Climate Change), 2006. *2006 IPCC Guidelines for National Greenhouse Gas Inventories, Volume 5, Waste* (Chapter 3). IGES.
22. JCGM 100:2008. (2008). *Guide to the expression of uncertainty in measurement*.
23. Jin, C., Sun, S., Yang, D., Sheng, W., Ma, Y., He, W., & Li, G. (2021). Anaerobic digestion: An alternative resource treatment option for food waste in China. *The Science of the Total Environment*, 779, 146397. <https://doi.org/10.1016/j.scitotenv.2021.146397>
24. Kamau, M. J., & Andati, W. G. (2025). Sustainable Management of Organic Waste in Municipalities: Pathways to Bio-Energy, Bio-Fertilizer Production, and Climate Action. *Journal of Environmental Ecology*, 1(1), 1–9. <https://doi.org/10.64229/xjnt7f33>

25. Kaza, S., Yao, L., Bhada-Tata, P., & Van Woerden, F. (2018). *What a Waste 2.0: A Global Snapshot of Solid Waste Management to 2050*. <https://doi.org/10.1596/978-1-4648-1329-0> [08/01/2025]
26. Kennedy, M. C., & O'Hagan, A. (2001). Bayesian calibration of computer models. *Journal of the Royal Statistical Society: Series B (Statistical Methodology)*, 63(3), 425–464. <https://doi.org/10.1111/1467-9868.00294>
27. Lange, K. L., Little, R. J. A., & Taylor, J. M. G. (1989). Robust Statistical Modeling Using the t Distribution. *Journal of the American Statistical Association*, 84(408), 881–896. <https://doi.org/10.1080/01621459.1989.10478852>
28. Limpert, E., Stahel, W. A., & Abbt, M. (2001). Log-normal Distributions across the Sciences: Keys and Clues: On the charms of statistics, and how mechanical models resembling gambling machines offer a link to a handy way to characterize log-normal distributions, which can provide deeper insight into variability and probability—normal or log-normal: That is the question. *BioScience*, 51(5), 341–352. [https://doi.org/10.1641/0006-3568\(2001\)051%255B0341:LNDATS%255D2.0.CO;2](https://doi.org/10.1641/0006-3568(2001)051%255B0341:LNDATS%255D2.0.CO;2)
29. Maasakkers, B., & Aben, I. (2025). *Targeting Waste emissions Observed from Space (TWOS)* [Dataset]. <https://www.sron.nl/en/pillars/science/earth/targeting-waste-emissions-observed-from-space/> [08/01/2025]
30. Md. Code Regs. 26.11.42, Control of Methane Emissions from Municipal Solid Waste Landfills (2022).
31. McGaughy, K., Morelli, B., Martell, A., Ana, J. S., & Ingwersen, W. W. (2024). Food waste end-of-life management for the United States: Parameterized life cycle inventory datasets. *Data in Brief*, 57, 111174. <https://doi.org/10.1016/j.dib.2024.111174>
32. Mexico National Institute of Statistics and Geography (INEGI). (2017). *National Census of Municipal and Delegational Governments* [Dataset]. <https://en.www.inegi.org.mx/> [08/01/2025]
33. Nocedal, J., & Wright, S. J. (2006). *Numerical Optimization*. Springer New York. <https://doi.org/10.1007/978-0-387-40065-5>
34. Oehlert, G. W. (1992). A Note on the Delta Method. *The American Statistician*, 46(1), 27–29. <https://doi.org/10.2307/2684406>
35. OpenStreetMap Foundation. (2025). *OpenStreetMap* (Version 2025) [Dataset]. <https://www.openstreetmap.org/#map=5/38.01/-95.84> [08/01/2025]
36. Pizzanelli, S., Calucci, L., Forte, C., & Borsacchi, S. (2023). Studies of Organic Matter in Composting, Vermicomposting, and Anaerobic Digestion by ^{13}C Solid-State NMR Spectroscopy. *Applied Sciences*, 13(5), 2900. <https://doi.org/10.3390/app13052900>
37. Poole, D., & Raftery, A. E. (2000). Inference for Deterministic Simulation Models: The Bayesian Melding Approach. *Journal of the American Statistical Association*, 95(452), 1244–1255. <https://doi.org/10.1080/01621459.2000.10474324>

38. Proost, J. H. (2019). Calculation of the Coefficient of Variation of Log-Normally Distributed Parameter Values. *Clinical Pharmacokinetics*, 58(9), 1101–1102. <https://doi.org/10.1007/s40262-019-00760-6>
39. Raniga, K., et al (2024). *Temporal Disaggregation of Emissions Data for the Climate TRACE Inventory* [Online]. Available at: <https://github.com/climatetracecoalition/methodology-documents/tree/main/2024/Post%20Processing%20for%20Global%20Emissions%20and%20Metadata%20Completeness> [Accessed: 15 November 2024]
40. RMI. (2025). *RMI/SWEET_python* [Python]. RMI. https://github.com/RMI/SWEET_python
41. Saltelli, A., Ratto, M., Andres, T., Campolongo, Francesca, Cariboni, J., Gatelli, D., Saisana, M., & Tarantola, S. (2007). Global Sensitivity Analysis. The Primer. In *Global Sensitivity Analysis. The Primer*. John Wiley & Sons, Ltd. <https://onlinelibrary.wiley.com/doi/abs/10.1002/9780470725184.ch6>
42. Scheutz, C., Cassini, F., De Schoenmaeker, J., & Kjeldsen, P. (2017). Mitigation of methane emissions in a pilot-scale biocover system at the AV Miljø Landfill, Denmark: 2. Methane oxidation. *Waste Management*, 63, 203–212. <https://doi.org/10.1016/j.wasman.2017.01.012>
43. Tierney, L., & Kadane, J. B. (1986). Accurate Approximations for Posterior Moments and Marginal Densities. *Journal of the American Statistical Association*, 81(393), 82–86. <https://doi.org/10.1080/01621459.1986.10478240>
44. Ulloa-Murillo, L. M., Villegas, L. M., Rodríguez-Ortiz, A. R., Duque-Acevedo, M., & Cortés-García, F. J. (2022). Management of the Organic Fraction of Municipal Solid Waste in the Context of a Sustainable and Circular Model: Analysis of Trends in Latin America and the Caribbean. *International Journal of Environmental Research and Public Health*, 19(10), 6041. <https://doi.org/10.3390/ijerph19106041>
45. UNEP. (2021). *International Methane Emissions Observatory (IMEO)* [Dataset]. <https://www.unep.org/topics/energy/methane/international-methane-emissions-observatory> [08/01/2025]
46. United Nations, Department of Economic and Social Affairs, Population Division. (2025). *UN Population Division Data Portal* [Dataset]. <https://population.un.org/dataportal/> [08/01/2025]
47. US EPA. (2022). *Basic Information about Landfill Gas*. <https://www.epa.gov/lmop/basic-information-about-landfill-gas>. [09/01/2022]
48. US EPA, O. (2022, January 26). *Apply Biofilters or Biocovers* <https://www.epa.gov/lmop/apply-biofilters-or-biocovers>
49. US EPA. (2025a). *Greenhouse Gas Reporting Program (GHGRP)* [Dataset]. <https://www.epa.gov/ghgreporting> [08/01/2025]
50. US EPA. (2025b). *Landfill Methane Outreach Program (Version 2025)* [Dataset]. <https://www.epa.gov/lmop> [08/01/2025]
51. US EPA (2025c). Solid Waste Emissions Estimation Tool (SWEET) *Global Methane Initiative*. <https://www.globalmethane.org/>.

52. van der Vaart, A. W. (Ed.). (1998). Delta Method. In *Asymptotic Statistics* (pp. 25–34). Cambridge University Press. <https://doi.org/10.1017/CBO9780511802256.004>
53. Wang, Y., Fang, M., Lou, Z., He, H., Guo, Y., Pi, X., Wang, Y., Yin, K., & Fei, X. (2024). Methane emissions from landfills differentially underestimated worldwide. *Nature Sustainability*, 7(4), 496–507. <https://doi.org/10.1038/s41893-024-01307-9>
54. Waste Atlas. (2013). *Waste Atlas* [Dataset]. <http://www.atlas.d-waste.com/> [08/01/2025]
55. World Biogas Association. (n.d.). *Report—Global potential of biogas | 2019*. Retrieved October 28, 2025, from https://www.worldbiogassassociation.org/wp-content/uploads/2019/09/WBA-globalreport-56ppa4_digital-Sept-2019.pdf
56. WorldClim. (2025). *WorldClim* [Dataset]. <https://www.worldclim.org/> [08/01/2025].